Research Article

Analysis of Passive Partial Shading Mitigation Technique for PV Array

Santosh B.S.S*[a,b], Mohamed Thameem Ansari.M[a], Kantarao.P[b]

[a] Department of Electrical Engineering, Annamalai University and Annamalai Nagar, P. O. Box: 608002, India.
[b] Department of Electrical Engineering, SRKREC and Bhimavaram, India.

ABSTRACT

In the present day, a significant portion of the world's energy demand can be satisfied through the utilization of renewable energy sources. Solar energy, in particular, holds a pivotal position owing to its numerous merits. However, it faces a challenge known as mismatch response within the photovoltaic (PV) modules of an array when subjected to partial shading. This issue restricts power output, leads to the formation of local hot spots, and results in the underutilization of PV modules within the array. One of the most effective solutions to address this problem is optimizing the PV array (PVA) configuration to maximize output power under partial shading (PS) conditions. In this research paper, we commence with a thorough numerical analysis under uniform shading conditions. Following that, we scrutinize the performance of six traditional PVA configurations and three hybrid PVA configurations under PS conditions. The results consistently indicate that the Total Cross Tied (TCT) configuration outperforms others in all shading scenarios in terms of mitigating mismatch power loss, enhancing the fill factor, and improving overall efficiency.

1. INTRODUCTION

Energy is absolutely necessary for the expansion and prosperity of the economy. Because of the swift acceleration of industrialization and the push toward economic expansion, the world has a massive demand for power (Husain 2018). These days, consumers around the world are demanding uninterrupted power supply. Many factors such as lack of fuel, load shedding, internal failures, and many other factors can cause disruption in a conventional electrical system. Therefore, the integration of renewable resources has become more popular, and their functions are to meet global demand (Krishna 2019). Among several renewable resources, solar energy gains greater importance because of its merits like abundance, eco-friendliness, and also advancements in semiconductor technology (Tatabhatla 2019). In spite of these merits, solar systems suffer from low efficiency, large susceptance to environmental changes, partial shading, and dust deposition, which leads to a reduction in the output power of the solar system. Among these, partial shading creates a huge impact on the system's efficiency. The key factors that contribute to partial shade conditions include tree shadows, towers and other structures, moving clouds, aging-related cell damage, bird droppings, and soiling (Harish Kumar Varma 2021). In order to get the correct voltage and current as required by the load, a large number of modules are connected in series and parallel to form the PV arrays. The electrical characteristics of shaded and unshaded panels differ under shading conditions, and this characteristic discrepancy increases as the illumination intensities change. The mismatching causes a drastic drop in

output power under real-world operating conditions. The amount of power lost due to shading depends on a number of variables, including the intensity of shading, where in the PV array the shaded panels are located, and, most crucially, the arrangement of the PV panels themselves.

Over the years, many partial shade mitigation strategies have been developed in order to extend the lifetime of PV modules as well as to maximize the amount of energy that can be harvested from solar PV modules. Despite having poor efficiency, these methods have allowed the PV system to be employed in systems for water pumping, commercial and residential buildings, electric vehicles, etc. There are primarily two categories for partial shade mitigation, which are 1) passive mitigation solutions, such as bypass diodes and PV array topologies, and 2) active mitigation methods, such as multilevel inverters, distributed MPPT approaches, and static and dynamic reconfiguration strategies. (i) According to the literature, the partial shading effects can be mitigated by: (i) Connection of bypass diodes (Bhadoria 2020) – which mitigates the formation of local hot spots but results in the formation of many peak power points on the I-V and P-V characteristics. Because of this, conventional maximum power point tracking (also known as MPPT) does not successfully track the global peak value. (ii) Usage of Global maximum power tracking techniques (Goud 2018) - Because of this, the total number of sensors in the system must be increased, as

must the cost of these sensors. Furthermore, this raises the computational difficulty and memory necessity. (iii) Distributed MPPT converter system (Zhou 2020) - Each PV module's power electronic converters with MPPT allow it to function at maximum power. However, the high number of converters needed raises the overall system price. (iv) Implementing PV array configuration scheme (Kho 2018) – In (F. Belhachat 2015), Comprehensive research on S, P, SP, TCT, BL, and HC topologies has been presented by the authors. Under conditions of partial shading, the authors found that the results unequivocally demonstrate that the performances of the various PV array configurations are variable and strongly depend on the intensity of shading, the shading pattern, the location of the shading pattern, and the type of shading that is affecting the PV array. It is concluded in (Okan Bingol 2018) that the T-C-T PV array topology generates the maximum power by mitigating the mismatching power losses due to a smaller number of series interconnections compared with S, P, S-P, T-C-T, B-L, and H-C topologies under uniform and various shading patterns like uneven row, uneven column, diagonal, and random shading patterns. The authors of (Prem kumar 2020) discussed the performance of the conventional and hybrid topologies and came to the conclusion that the TCT configuration was superior to the other topologies in terms of delivering the highest output power. In this paper, Conventional and Hybrid configurations are analyzed using a 6×6 PV array using the SunPower SPR-76R-BLK-U PV module, and specifications are mentioned in Table - 1. The main objective of this research work is,

- Mathematical representation of conventional and hybrid topologies in partial shading.
- Analyze conventional and hybrid topologies by shading factor, operating panels, array voltage, array current, and array power at each string voltage interval.
- Economic study of conventional and hybrid topologies.

This paper is arranged as follows: Section 2 analyzes TCT PV Array Configurations under uniform shading condition. Section 3 represents the numerical analysis of PVA configuration under different shading conditions. Section 4 compares conventional and hybrid PV array configurations for different shading conditions, including performance and economic analysis. Finally, section 5 ends with a conclusion.

Table 1. Specifications of SunPower SPR-76R-BLK-U PV module

S. no	Specifications	Values
1	Peak Power (P_{Pe})	76.275 (W)
2	Open circuit voltage (V_{OC})	16.2 (V)
3	Short-circuit current (I_{SC})	6.02 (A)
4	Peak power point voltage (V_{pe})	13.5 (V)
5	Peak power point current (I_{pe})	5.65 (A)
6	Module area (A)	0.54 (m^2)

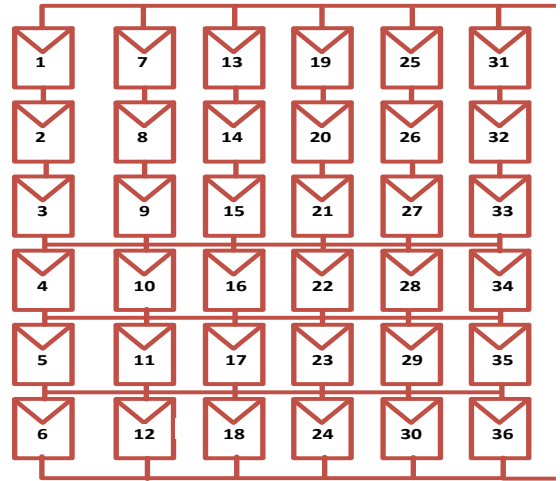## 2. CONFIGURATIONS AND SHADING PATTERNS
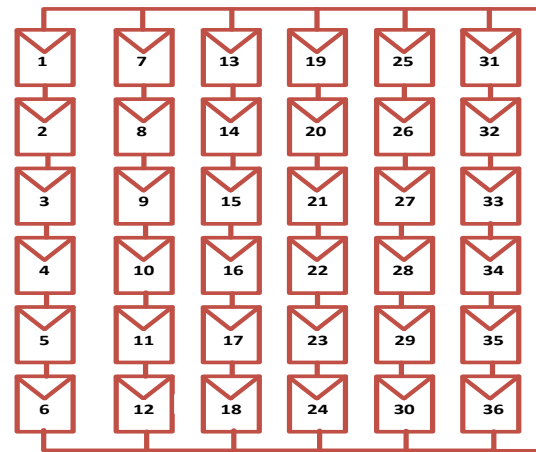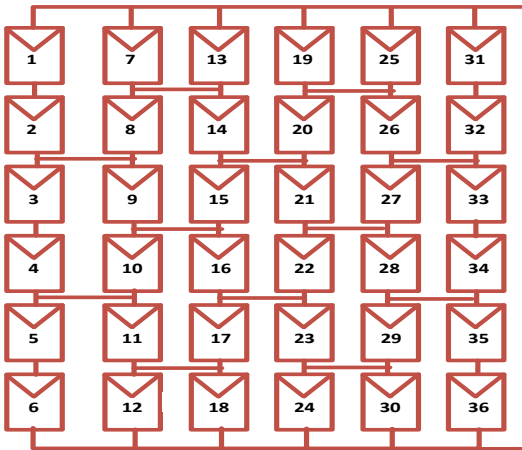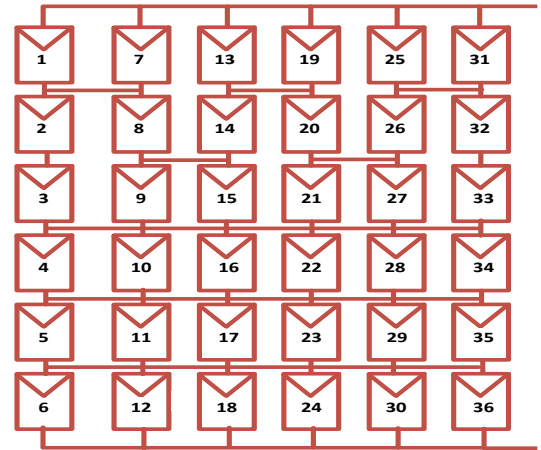

(a) SP

(b) TCT

(c) LD
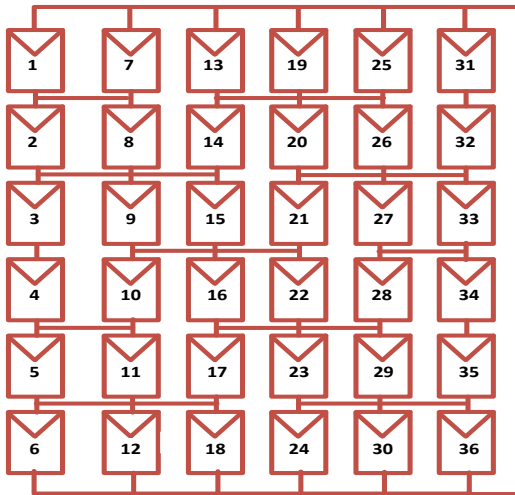
(d) TrCT

(g) SPTCT

(e) BL

(h) BLTCT
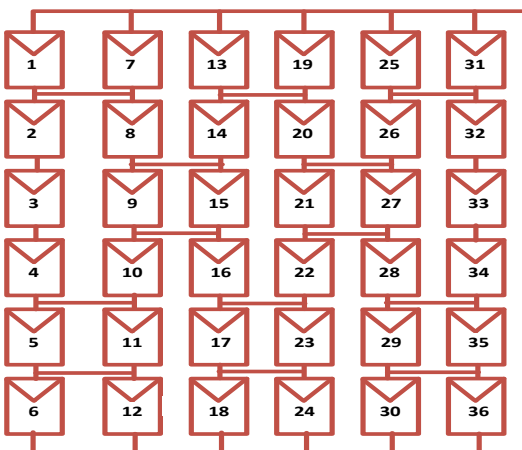
(f) HC
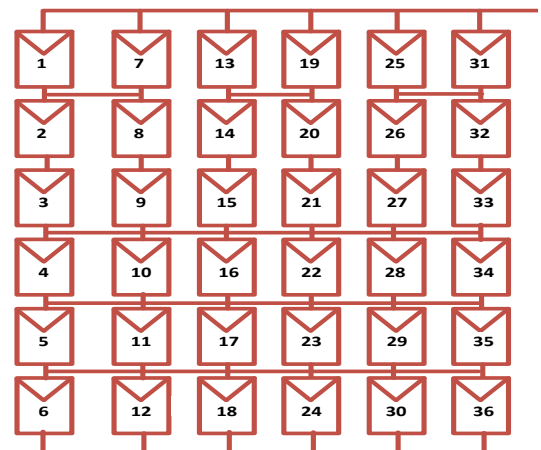
(i) HCTCT

Figure 1. PV Array Configurations

300	1000	1000	1000	1000	1000
1000	400	1000	1000	1000	1000
1000	1000	500	1000	1000	1000
1000	1000	1000	600	1000	1000
1000	1000	1000	1000	700	1000
1000	1000	1000	1000	1000	800

(a) Diagonal (DIA)

1000	1000	1000	1000	1000	1000
1000	1000	1000	1000	1000	1000
1000	1000	1000	1000	1000	1000
1000	1000	1000	1000	1000	1000
200	400	1000	1000	1000	1000
600	800	1000	1000	1000	1000

(b) Short Narrow (SN)

1000	1000	1000	1000	1000	1000
1000	1000	1000	1000	1000	1000
1000	1000	1000	1000	1000	1000
1000	1000	1000	1000	1000	1000
200	400	600	800	1000	1000
100	300	500	700	1000	1000

(c) Short Wide (SW)

1000	1000	1000	1000	1000	1000
1000	1000	1000	1000	1000	1000
200	300	1000	1000	1000	1000
400	500	1000	1000	1000	1000
600	700	1000	1000	1000	1000
800	900	1000	1000	1000	1000

(d) Long Narrow (LN)

1000	1000	1000	1000	1000	1000
1000	1000	1000	1000	1000	1000
200	300	400	500	1000	1000
600	700	800	900	1000	1000
200	300	400	500	1000	1000
600	700	800	900	1000	1000

(e) Long Wide (LW)

Figure 2. Shading Patterns

In this work, six conventional PVA configurations such as Series Parallel (SP), Total Cross Tied (TCT), Bridge Link (BL), Honey Comb (HC), Ladder (LD), Triple Cross Tied (TrCT) and three hybrid PVA configurations such as Series Parallel - Total Cross Tied (SPTCT), Bridge Link - Total Cross Tied (BLTCT), Honey Comb - Total Cross Tied (HCTCT) configurations are considered, as shown in Fig 1. The mentioned PVA configurations are analyzed under diagonal (DIA), short narrow (SN), short wide (SW), long narrow (LN) and long wide (LW) shading conditions, as shown in Fig 2.

2.1 Numerical representation of TCT Configurations under uniform shading

The equivalent photo current under the unshaded condition, I_{USH} is expressed as

$$I_{USH} = I_L \times \frac{G}{G_{STC}} \approx I_{SC} \times \frac{G}{G_{STC}} \qquad (1)$$

where I_L, G_{STC} : Photo current and Irradiance in Standard Test Conditions (STC) & $G_{STC} = 1000$ W/m²; G: Irradiance falling on the module under shading condition, I_{SC}: Short circuit current of the PV Module.

The equivalent photo current under the shaded condition, I_{SH} is expressed as

$$I_{SH} = I_L \times \frac{G_{SH}}{G_{STC}} = I_L \times \frac{(1-\beta)G}{G_{STC}} = I_{USH} - \left(\frac{G \times \beta}{G_{STC}} \times I_L \right) \qquad (2)$$

where β: Shading factor and it is expressed as $\beta = 1 - \frac{G_{SH}}{G}$

and G_{SH}: Irradiance on shading condition

2.1.1 TCT configuration under the Diagonal (DIA) shading condition:

As can be seen in Figure 3, diagonal modules, i.e., 1,8,15,22,29 and 36, are under the shading condition and it is assumed that shading intensity is 600 W/m², meaning that β = 0.4.
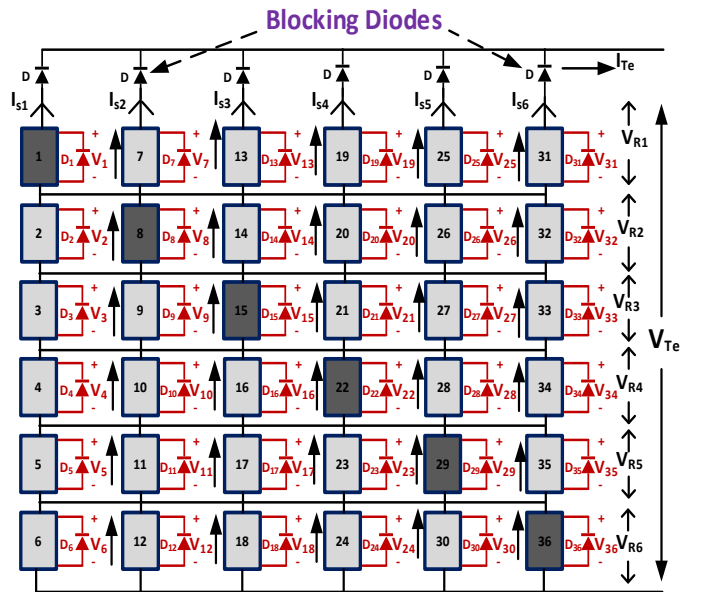
Figure 3. TCT configuration under diagonal shading

From the equivalent circuit of PV module (S.R.Pendem 2018), (AA. Desai 2021) the unshaded module current (I_A) and shaded module current (I_B) are expressed as

$$I_A = I_{USH} - I_o \left[\exp \left(\frac{q \times V_{USH}}{nKT} \right) - 1 \right] \qquad (3)$$

Where (V, I) $_{USH}$ = Voltage & Currents of the Unshaded modules = (V, I)$_{2-6, 7, 9-12, 13,14, 16-18, 19-21, 23,24, 25-28,30, 31-35}$ (4)

Similarly:

$$I_B = I_{SH} - I_o \left[\exp \left(\frac{q \times V_{SH}}{nKT} \right) - 1 \right] \qquad (5)$$

Where (V, I) $_{SH}$ = Voltage & Currents of the Shaded modules = (V, I)$_{1,8,15,22,29,36}$ (6)

From Fig (4), the array current (I_{Te}) is expressed as:

$$I_{Te} = I_{s1} + I_{s2} + I_{s3} + I_{s4} + I_{s5} + I_{s6} \qquad (7)$$

where

$I_{s1} = I_1 = I_2 = I_3 = I_4 = I_5 = I_6$; $I_{s2} = I_7 = I_8 = I_9 = I_{10} = I_{11} = I_{12}$; $I_{s3} = I_{13} = I_{14} = I_{15} = I_{16} = I_{17} = I_{18}$; $I_{s4} = I_{19} = I_{20} = I_{21} = I_{22} = I_{23} = I_{24}$; $I_{s5} = I_{25} = I_{26} = I_{27} = I_{28} = I_{29} = I_{30}$; $I_{s6} = I_{31} = I_{32} = I_{33} = I_{34} = I_{35} = I_{36}$ $\qquad$ (8)

and the row voltages can be expressed as,

$V_{R1} = V_1 = V_7 = V_{13} = V_{19} = V_{25} = V_{31}$; $V_{R2} = V_2 = V_8 = V_{14} = V_{20} = V_{26} = V_{32}$; $V_{R3} = V_3 = V_9 = V_{15} = V_{21} = V_{27} = V_{33}$; $V_{R4} = V_4 = V_{10} = V_{16} = V_{22} = V_{28} = V_{34}$; $V_{R5} = V_5 = V_{11} = V_{17} = V_{23} = V_{29} = V_{35}$; $V_{R6} = V_6 = V_{12} = V_{18} = V_{24} = V_{30} = V_{36}$ $\qquad$ (9)

From Eq. (7) and Eq. (8),

$$I_{Te} = I_1 + I_7 + I_{13} + I_{19} + I_{25} + I_{31} \quad = I_B + 5\,I_A \qquad (10)$$

$$= I_{SH} - I_o\left[\exp\left(\frac{q \times V_1}{nKT}\right) - 1\right] + I_{USH} - I_o\left[\exp\left(\frac{q \times V_{7,13,19,25,31}}{nKT}\right) - 1\right]$$

$$= I_{USH} - \left(\frac{G \times \beta}{G_{STC}} \times I_L\right) - I_o\left[\exp\left(\frac{q \times V_1}{nKT}\right) - 1\right] + I_L \times \frac{G}{G_{STC}} - I_o\left[\exp\left(\frac{q \times V_{7,13,19,25,31}}{nKT}\right) - 1\right] \qquad (11)$$

From Eq. (9) and Eq. (11), the modified (I_{Te}) is given as

$$= 6I_L\left(\frac{G}{G_{STC}}\right) - \left(\frac{G \times \beta}{G_{STC}} \times I_L\right) - 6I_o\left[\exp\left(\frac{q \times V_1}{nKT}\right) - 1\right] \quad (12)$$

Similarly

$$V_1 = V_2 = V_3 = V_4 = V_5 = V_6 = \frac{nKT}{q} \times \ln\left[\frac{6I_L\left(\frac{G}{G_{STC}}\right) - \left(\frac{G \times \beta}{G_{STC}} \times I_L\right) - I_{Te}}{6I_o} + 1\right] \qquad (13)$$

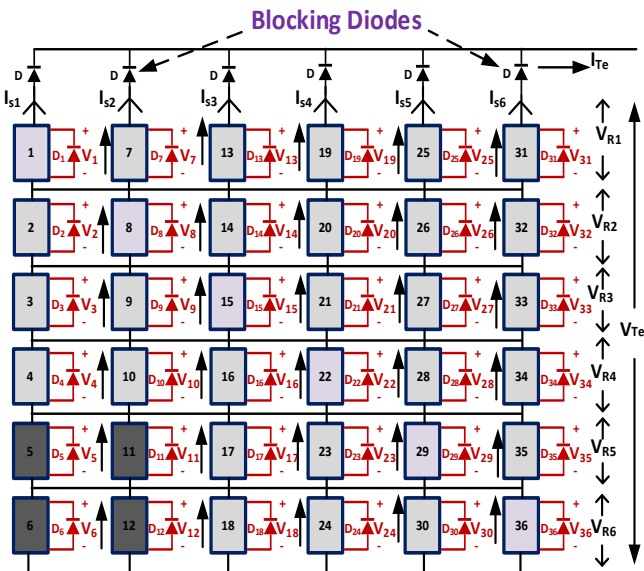## 2.1.2 TCT configuration under Short Narrow (SN) shading condition:

Figure 4. TCT configuration under Short Narrow (SN) shading

Based on the shading condition shown in Figure 4, the total array current can be divided into unshaded row current (I_{Te})$_{ush}$ and shaded row current (I_{Te})$_{sh}$.

$$I_{Te,ush} = I_1 + I_7 + I_{13} + I_{19} + I_{25} + I_{31} = I_{USH} - I_o\left[\exp\left(\frac{q \times V_1}{nKT}\right) - 1\right] \qquad (14)$$

and $\quad I_{Te,sh} = I_5 + I_{11} + I_{17} + I_{23} + I_{29} + I_{35}$

$= I_{USH} - \left(\frac{G \times \beta}{G_{STC}} \times I_L\right) - I_o\left[\exp\left(\frac{q \times V_5}{nKT}\right) - 1\right] + I_{USH} - \left(\frac{G \times \beta}{G_{STC}} \times I_L\right) - I_o\left[\exp\left(\frac{q \times V_{11}}{nKT}\right) - 1\right] + I_{USH} - \left(\frac{G \times \beta}{G_{STC}} \times I_L\right) - I_o\left[\exp\left(\frac{q \times V_{17}}{nKT}\right) - 1\right] + I_{USH} - \left(\frac{G \times \beta}{G_{STC}} \times I_L\right) - I_o\left[\exp\left(\frac{q \times V_{23}}{nKT}\right) - 1\right] + I_{USH} - \left(\frac{G \times \beta}{G_{STC}} \times I_L\right) - I_o\left[\exp\left(\frac{q \times V_{29}}{nKT}\right) - 1\right] + I_{USH} - \left(\frac{G \times \beta}{G_{STC}} \times I_L\right) - I_o\left[\exp\left(\frac{q \times V_{35}}{nKT}\right) - 1\right]$

From Eq. (9), $I_{Te,sh}$ can be rewritten as

$$I_{Te,sh} = 6I_{USH} - \left(\frac{2G \times \beta}{G_{STC}} \times I_L\right) - 6I_o\left[\exp\left(\frac{q \times V_5}{nKT}\right) - 1\right] \qquad (15)$$

Similarly, from Eq. (14) and Eq. (15), we have:

$$V_1 = V_2 = V_3 = V_4 = \frac{nKT}{q} \times \ln\left[\frac{6I_L\left(\frac{G}{G_{STC}}\right) - I_{Te,ush}}{6I_o} + 1\right] \quad (16)$$

$$V_5 = V_6 = \frac{nKT}{q} \times \ln\left[\frac{6I_{USH} - \left(\frac{2G \times \beta}{G_{STC}} \times I_L\right) - I_{Te,sh}}{6I_o} + 1\right] \qquad (17)$$

From Eqs. (12,13) and Eqs. (15-17), the short circuit current (I_{sc}) and the point at which I-V curve changes its path (I_{cp}), number of maximum values for $\beta = 0.4$ and $G = 1000$ W/m^2 are mentioned in Table 2 and simulated results are shown in Figure 5. In addition, the same analysis is extended for the remaining shading patterns.

Table 2. Numerical analysis results of TCT configuration in the uniform shading condition

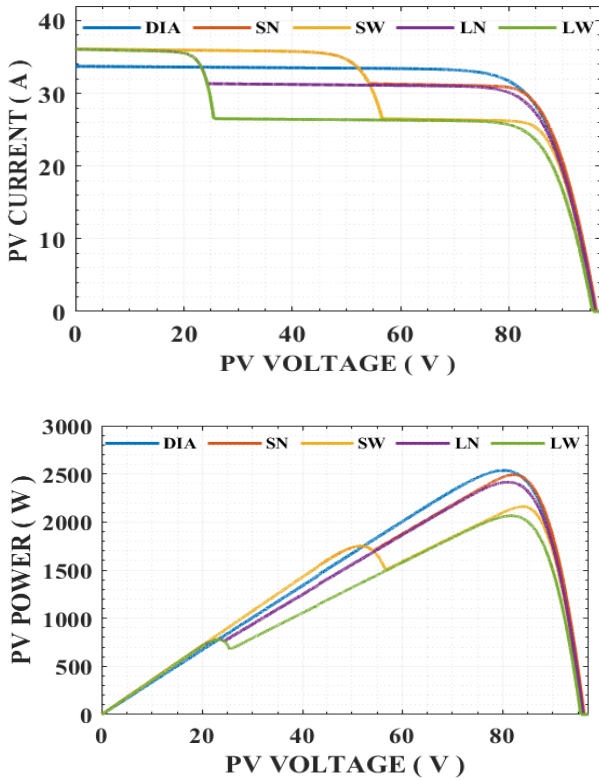| Topology	Shading Pattern	I_{sc} (A)	I_{cp} (A)	Maximum Values
	DIA	$6I_{sc} - 2\,\beta\,I_{sc}$	--	1
	SN	$6I_{sc}$	$6I_{sc} - 2\,\beta\,I_{sc}$	2
TCT	SW	$6I_{sc}$	$6I_{sc} - 4\,\beta\,I_{sc}$	2
	LN	$6I_{sc}$	$6I_{sc} - 2\,\beta\,I_{sc}$	2
	LW	$6I_{sc}$	$6I_{sc} - 4\,\beta\,I_{sc}$	2

Figure 5. Output characteristics of TCT Configurations for β = 0.4

3. NUMERICAL ANALYSIS OF PV ARRAY CONFIGURATIONS UNDER PARTIAL SHADING CONDITONS

6 x 6 PVA topologies are simulated in the MATLAB/Simulink software under 5 partial shade situations, and numerical analysis is conducted in terms of the working modules, peak voltage (V_{pe}), peak current (I_{pe}), and peak power (P_{pe}) as mentioned in Table [3-11].

3.1 Series-Parallel (SP) Configuration:

This configuration aims to balance the benefits of both series and parallel connections. The array is divided into smaller sub-arrays connected in parallel, with each sub-array having multiple modules connected in series. This configuration reduces the impact of shading on the entire array. If one sub-array is shaded, only that sub-array's performance is significantly affected, while other sub-arrays continue to operate at a higher efficiency. This allows the unaffected sub-arrays to contribute more the overall power output, reducing the performance loss caused by shading. The MATLAB simulation connection is shown in Figure 6, and the simulated I-V and P-V curves are presented in Figure 7.

Figure 6. Simulink® connection diagram for the configuration of the SP PV array

Table 3. Representation of PV array parameters for SP Configuration under various shading conditions

Shading Scheme	Interval at which Array Voltage, Current and Power change		
DIA	$0 \leq V_{Te} \leq 5V_{Pe}$	$5V_{Pe} \leq V_{Te} \leq 6V_{Pe}$	
Working modules	2-6, 7,9-12,13,14,16-18, 19-21,23,24,25-28,30, 31-35	1,8,15,22,29,36	
V_{Te}	5 V_{Pe}	6 V_{Pe}	
I_{Te}	6 I_{Pe}	3.3 I_{Pe}	
P_{Te}	**30 $V_{Pe} I_{Pe}$**	19.8 $V_{Pe} I_{Pe}$	
SN	$0 \leq V_{Te} \leq 4V_{Pe}$	$4V_{Pe} \leq V_{Te} \leq 5V_{Pe}$	$5V_{P} \leq V_{Te} \leq 6V_{Pe}$
Working modules	1-4,7-10,13-36	2,12,13-36	5,11, 13-36
V_{Te}	4 V_{Pe}	5 V_{Pe}	6 V_{Pe}
I_{Te}	6 I_{Pe}	5.4 I_{Pe}	4.4 I_{Pe}
P_{Te}	24 $V_{Pe} I_{Pe}$	**27 $V_{P} I_{Pe}$**	26.4 $V_{Pe} I_{Pe}$
SW	$0 \leq V_{Te} \leq 4V_{Pe}$	$4V_{Pe} \leq V_{Te} \leq 5V_{Pe}$	$5V_{Pe} \leq V_{Te} \leq 6V_{Pe}$

Shading Scheme	Interval at which Array Voltage, Current and Power change				
Working modules	1-4,7-10,13-16,19-22,25-36			5,11,17,23,25-36	6,12,18,24,25-36
V_{Te}	4 V_{Pe}			5 V_{Pe}	6 V_{Pe}
I_{Te}	6 I_{Pe}			4 I_{Pe}	3.6 I_{Pe}
P_{Te}	**24 $V_{Pe}I_{Pe}$**			20 $V_{Pe}I_{Pe}$	21.6 $V_{Pe}I_{Pe}$
LN	$0 \leq V_{Te} \leq 2V_{Pe}$	$2V_{Pe} \leq V_{Te} \leq 3V_{Pe}$	$3V_{Pe} \leq V_{Te} \leq 4V_{Pe}$	$4V_{Pe} \leq V_{Te} \leq 5V_{Pe}$	$5V_{Pe} \leq V_{Te} \leq 6V_{Pe}$
Working modules	1,2,7,8,13-36	1,2,6,7,8,12,13-36	5,6,11,12,13-36	4,10,13-36	3,9,13-36
V_{Te}	2V_{Pe}	3 V_{Pe}	4 V_{Pe}	5 V_{Pe}	6 V_{Pe}
I_{Te}	6 I_{Pe}	5.8 I_{Pe}	5.4 I_{Pe}	5 I_{Pe}	4.4 I_{Pe}
P_{Te}	12 $V_{Pe}I_{Pe}$	17.4 $V_P I_P$	21.6 $V_{Pe}I_{Pe}$	25 $V_{Pe}I_{Pe}$	**26.4 $V_{Pe}I_{Pe}$**
LW	$0 \leq V_{Te} \leq 2V_{Pe}$	$2V_{Pe} \leq V_{Te} \leq 4V_{Pe}$		$4V_{Pe} \leq V_{Te} \leq 6V_{Pe}$	
Working modules	1,2,7,8,13,14,19,20,25-36	4,6,10,12,16,18,22,24,25-36		3,5,9,11,15,17,21,23,25-36	
V_{Te}	2V_{Pe}	4 V_{Pe}		6 V_{Pe}	
I_{Te}	6 I_{Pe}	5.1I_{Pe}		3.4 I_{Pe}	
P_{Te}	12 $V_{Pe}I_{Pe}$	20.4 $V_{Pe}I_{Pe}$		**20.4 $V_{Pe}I_{Pe}$**	

Figure 7. (a) Output Power - Voltage Curve (b) Output Current - Voltage Curve of SP Configuration

The number of local peaks generated is 1, 2, 2, 4, and 2 under DIA, SN, SW, LN, and LW shading conditions, respectively, and the global peak of 30 $V_{pe}I_{pe}$ is produced by the SP configuration under diagonal shading conditions, as mentioned in Table 3.

3.2 Total Cross Tied (TCT) PV array configuration:

The Total Cross Tied (TCT) PV array configuration, also known as Full Cross Tied or Fully Cross Tied, is a layout design used in photovoltaic (PV) systems. In a TCT configuration, each module is connected in both series and parallel to its neighboring modules. In a TCT configuration, each module has multiple parallel paths, and bypass diodes are often strategically placed within each module to allow current to flow around shaded modules. This helps prevent the shaded module from significantly affecting the entire string's performance. The MATLAB simulation connection is shown in Figure 8, and the simulated I-V and P-V curves are presented in Figure 9.
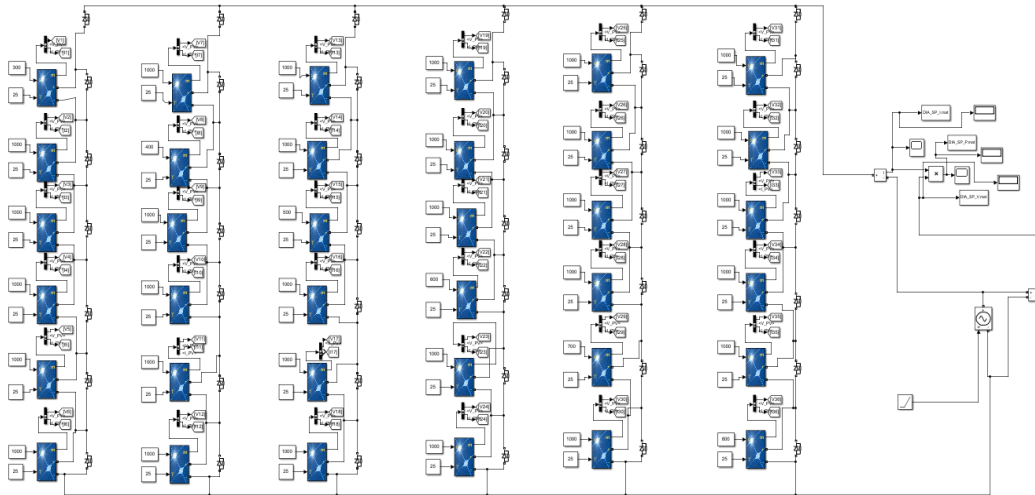

Figure 8. Simulink® connection diagram for the configuration of the TCT PV array

Table 4. Representation of PV array parameters for TCT Configuration under various shading conditions

Shading Scheme	Interval at which Array Voltage, Current and Power change					
DIA	$0 \le V_{Te} \le V_{Pe}$	$V_P \le V_{Te} \le 2V_{Pe}$	$2V_P \le V_{Te} \le 3 V_{Pe}$	$3 V_{Pe} \le V_{Te} \le 4 V_{Pe}$	$4 V_{Pe} \le V_{Te} \le 5 V_{Pe}$	$5 V_{Pe} \le V_{Te} \le 6 V_{Pe}$
Working modules	6,12,18,24,30,36	5,11,17,23,29,35	4,10,16,22,28,34	3,9,15,21,27,33	2,8,14,20,26,32	1,7,13,19,25,31
V_{Te}	V_{Pe}	$2 V_{Pe}$	$3 V_{Pe}$	$4 V_{Pe}$	$5 V_{Pe}$	$6 V_{Pe}$
I_{Te}	$5.8 I_{Pe}$	$5.7 I_{Pe}$	$5.6 I_{Pe}$	$5.5 I_{Pe}$	$5.4 I_{Pe}$	$5.3 I_{Pe}$
P_{Te}	$5.8 V_{Pe} I_{Pe}$	$11.4 V_{Pe} I_{Pe}$	$16.8 V_{Pe} I_{Pe}$	$22 V_{Pe} I_{Pe}$	$27 V_{Pe} I_{Pe}$	**$31.8 V_{Pe} I_{Pe}$**
SN	$0 \le V_{Te} \le 4V_{Pe}$				$4V_{Pe} \le V_{Te} \le 5V_{Pe}$	$5V_{Pe} \le V_{Te} \le 6V_{Pe}$
Working modules	1-4,7-10,13-16,19-22,25-28,31-34				6,12,18,24,30,36	5,11,17,23,29,35
V_{Te}	$4 V_{Pe}$				$5 V_{Pe}$	$6 V_{Pe}$
I_{Te}	$6 I_{Pe}$				$5.6 I_{Pe}$	$4.8 I_{Pe}$
P_{Te}	$24 V_{Pe} I_{Pe}$				$28 V_{Pe} I_{Pe}$	**$28.8 V_{Pe} I_{Pe}$**
SW	$0 \le V_{Te} \le 4V_{Pe}$				$4V_{Pe} \le V_{Te} \le 5V_{Pe}$	$5V_{Pe} \le V_{Te} \le 6V_{Pe}$
Working modules	1-4,7-10,13-16,19-22,25-28,31-34				5,11,17,23,29,35	6,12,18,24,30,36
V_{Te}	$4 V_{Pe}$				$5 V_{Pe}$	$6 V_{Pe}$
I_{Te}	$6 I_{Pe}$				$4.2 I_{Pe}$	$3.8 I_{Pe}$
P_{Te}	**$24 V_{Pe} I_{Pe}$**				$21 V_{Pe} I_{Pe}$	$22.8 V_{Pe} I_{Pe}$
LN	$0 \le V_{Te} \le 2V_{Pe}$	$2V_{Pe} \le V_{Te} \le 3V_{Pe}$	$3V_{Pe} \le V_{Te} \le 4V_{Pe}$	$4V_{Pe} \le V_{Te} \le 5V_{Pe}$	$5V_{Pe} \le V_{Te} \le 6V_{Pe}$	
Working modules	1,2,7,8,13,14,19,20,25,26,31,32	6,12,18,24,30,36	5,11,17,23,29,35	4,10,16,22,28,34	3,9,15,21,27,33	
V_{Te}	$2V_{Pe}$	$3 V_{Pe}$	$4 V_{Pe}$	$5 V_{Pe}$	$6 V_{Pe}$	
I_{Te}	$6 I_{Pe}$	$5.9 I_{Pe}$	$5.4 I_{Pe}$	$5.1 I_{Pe}$	$4.6 I_{Pe}$	
P_{Te}	$12 V_{Pe} I_{Pe}$	$17.7 V_{Pe} I_{Pe}$	$21.6 V_{Pe} I_{Pe}$	$25.5 V_{Pe} I_{Pe}$	**$27.6 V_{Pe} I_{Pe}$**	
LW	$0 \le V_{Te} \le 2V_{Pe}$	$2V_{Pe} \le V_{Te} \le 3V_{Pe}$	$3V_{Pe} \le V_{Te} \le 4V_{Pe}$	$4V_{Pe} \le V_{Te} \le 5V_{Pe}$	$5V_{Pe} \le V_{Te} \le 6V_{Pe}$	
Working modules	1,2,7,8,13,14,19,20,25,26,31,32	4,6,10,12,16,18,22,24,28,30,34,36		3,5,9,11,15,17,21,23,27,29,33,35		
V_{Te}	$2V_{Pe}$	$4 V_{Pe}$		$6 V_{Pe}$		
I_{Te}	$6 I_{Pe}$	$5.1 I_{Pe}$		$3.4 I_{Pe}$		
P_{Te}	$12 V_{Pe} I_{Pe}$	$20.4 V_{Pe} I_{Pe}$		**$20.4 V_{Pe} I_{Pe}$**		

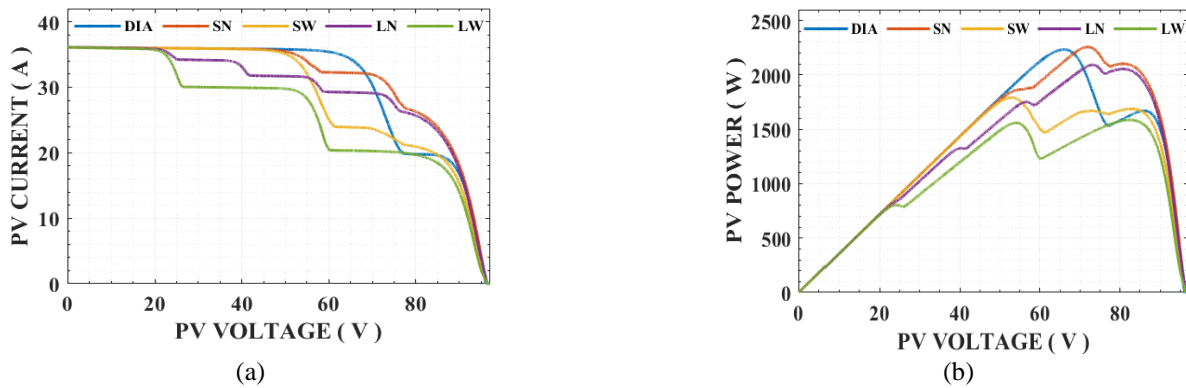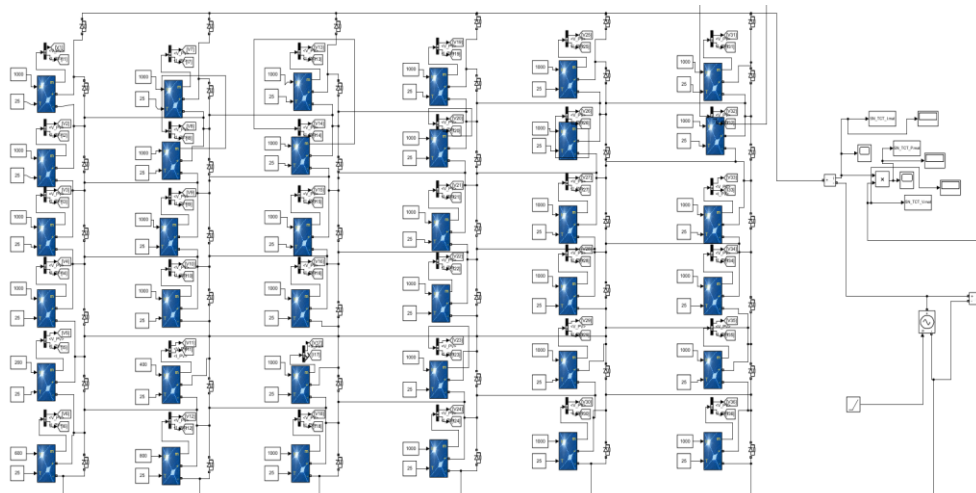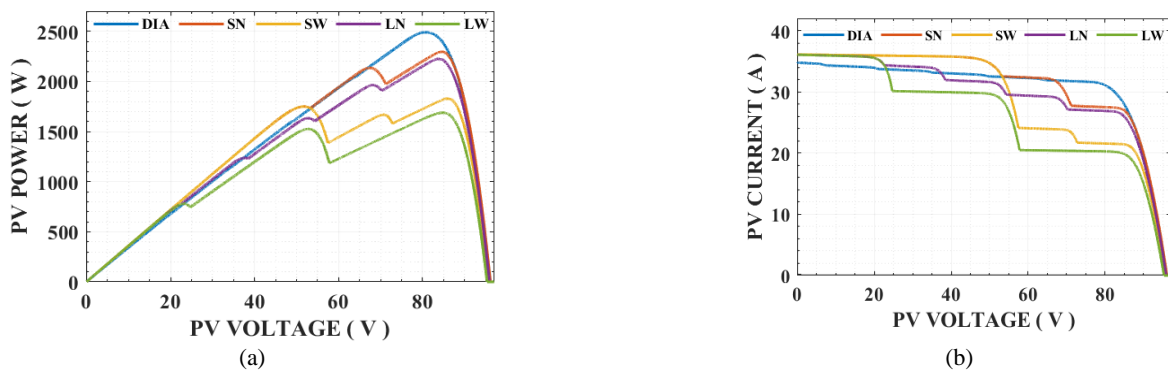**Figure 9.** (a) Output Power - Voltage Curve; (b) Output - Voltage Curve of TCT Configuration

The number of local peaks generated is 1, 2, 2, 4, and 2 under DIA, SN, SW, LN, and LW shading conditions, respectively, and the global peak of 30 $V_{pe}I_{pe}$ is produced by the SP configuration under diagonal shading conditions, as mentioned in Table 3.

3.3 Bridge – Link (BL) PV Array Configuration

The Total Cross Tied (TCT) PV array configuration, also known as Full Cross Tied or Fully Cross Tied, is a layout design used in photovoltaic (PV) systems. In a TCT configuration, each module is connected in both series and parallel to its neighboring modules. In a TCT configuration, each module has multiple parallel paths, and bypass diodes are often strategically placed within each module to allow current to flow around shaded modules. This helps prevent the shaded module from significantly affecting the entire string's performance. The MATLAB **simulation** connection is shown in Figure 8, and the simulated I-V and P-V curves are presented in Figure 9.

The number of local peaks generated is 1, 2, 2, 4, and 2 under DIA, SN, SW, LN, and LW shading conditions, respectively, with a global peak of 30 $V_{pe}I_{pe}$ produced by the BL configuration under diagonal shading conditions, as mentioned in Table 5.
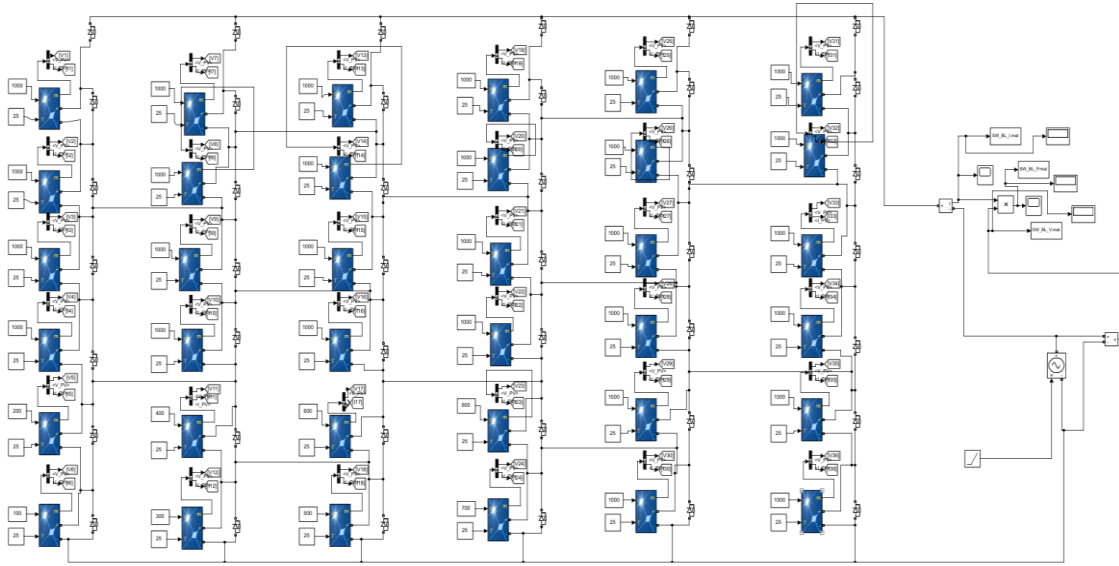
Figure 10. Simulink® connection diagram for the configuration of the BL PV array

Table 5. Representation of PV array parameters for BL Configuration under various shading conditions

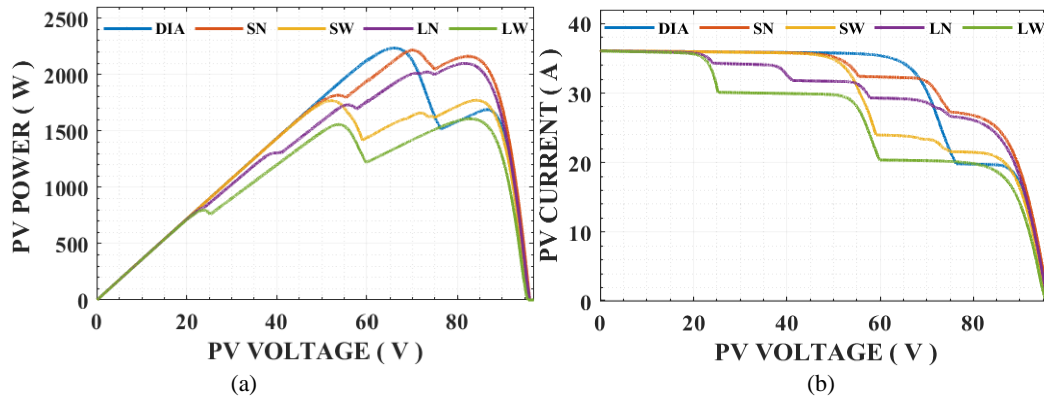| Shading Scheme	Interval at which Array Voltage, Current and Power change				
DIA	$0 \le V_{Te} \le 5V_{Pe}$				$5V_{Pe} \le V_{Te} \le 6V_{Pe}$
Working modules	2-6, 7,9-12,13,14,16-18, 19-21,23,24,25-28,30, 31-35				1,8,15,22,29,36
V_{Te}	$5V_{Pe}$				$6V_{Pe}$
I_{Te}	$6 I_{Pe}$				$3.3 I_{Pe}$
P_{Te}	**30 $V_{Pe} I_{Pe}$**				19.8 $V_{Pe} I_{Pe}$
SN	$0 \le V_{Te} \le 4V_{Pe}$			$4V_{Pe} \le V_{Te} \le 5V_{Pe}$	$5V_{Pe} \le V_{Te} \le 6V_{Pe}$
Working modules	1-4,7-10,13-17,19-36			6,12,16-18, 19-36	5,11,16,17,21-24,26-30,31-36
V_{Te}	$4 V_{Pe}$			$5 V_{Pe}$	$6 V_{Pe}$
I_{Te}	$6 I_{Pe}$			$5.6 I_{Pe}$	$4.6 I_{Pe}$
P_{Te}	24 $V_{Pe} I_{Pe}$			**28 $V_P I_{Pe}$**	27.6 $V_{Pe} I_{Pe}$
SW	$0 \le V_{Te} \le 4V_P$			$4V_P \le V_{Te} \le 5V_P$	$5V_P \le V_{Te} \le 6V_P$
Working modules	1-4,7-10,13-16,19-22,25-29,31-36			5,11,17,23,28,29,33-36	6,12,18,24,30,36
V_{Te}	$4 V_{Pe}$			$5 V_{Pe}$	$6 V_{Pe}$
I_{Te}	$6 I_{Pe}$			$4.1 I_{Pe}$	$3.7 I_{Pe}$
P_{Te}	**24 $V_{Pe} I_{Pe}$**			20.5 $V_{Pe} I_{Pe}$	22.2 $V_{Pe} I_{Pe}$
LN	$0 \le V_{Te} \le 2V_{Pe}$	$2V_{Pe} \le V_{Te} \le 3V_{Pe}$	$3V_{Pe} \le V_{Te} \le 4V_{Pe}$	$4V_{Pe} \le V_{Te} \le 5V_{Pe}$	$5V_{Pe} \le V_{Te} \le 6V_{Pe}$
Working modules	1,2,7,8,13,14,15,19-22,25-29, 31-36	6,12,14,15,18,19-36,	5,11,14-17,19-36	4,10,14-17,19-36	3,9,14,15,19-36
V_{Te}	$2V_{Pe}$	$3 V_{Pe}$	$4 V_{Pe}$	$5 V_{Pe}$	$6 V_{Pe}$
I_{Te}	$6 I_{Pe}$	$5.8 I_{Pe}$	$5.4 I_{Pe}$	$4.7 I_{Pe}$	$4.5 I_{Pe}$
P_{Te}	12 $V_{Pe} I_{Pe}$	17.4 $V_{Pe} I_{Pe}$	21.6 $V_{Pe} I_{Pe}$	23.5 $V_{Pe} I_{Pe}$	**27 $V_{Pe} I_{Pe}$**
LW	$0 \le V_{Te} \le 2V_{Pe}$	$2V_{Pe} \le V_{Te} \le 4V_{Pe}$		$4V_{Pe} \le V_{Te} \le 6V_{Pe}$	
Working modules	1,2,7,8,13,14,19,20,25-27,31-34	4,6,10,12,16,18,22,24,26-30,31-36		3,5,9,11,15,17,21,23,26-29,31-36	
V_{Te}	$2V_{Pe}$	$4 V_{Pe}$		$6 V_{Pe}$	
I_{Te}	$6 I_{Pe}$	$5.1 I_{Pe}$		$3.4 I_{Pe}$	
P_{Te}	12 $V_{Pe} I_{Pe}$	20.4 $V_{Pe} I_{Pe}$		**20.4 $V_{Pe} I_{Pe}$**	

Figure 11. (a) Output Power - Voltage Curve (b) Output Current - Voltage Curve of BL Configuration

3.4 Honey Comb (HC) PV Array Configuration

The drawbacks associated with Series-Parallel (SP) PV array configurations can be mitigated by adopting an arrangement that resembles the hexagonal pattern found in honeycomb architecture. This arrangement demonstrates improved performance in situations with uneven array sizes or when the number of module rows is fewer than the parallel strings receiving the same irradiance. The honeycomb (HC) configuration features a greater number of series-connected modules per string compared to TCT and BL arrangements while presenting a lesser number of series-connected modules per string in comparison to the SP configuration. Consequently, this results in a comparatively higher power loss due to mismatches than observed in TCT and BL configurations, but the extent of this loss is comparatively lower when compared to the SP configuration. The MATLAB simulation connection is shown in Figure 12, and the simulated I-V and P-V curves are presented in Figure 13.

The number of local peaks generated is 4, 2, 2, 4, and 2 under DIA, SN, SW, LN, and LW shading conditions, respectively, with the global peak of 28 VpeIpe produced by the HC configuration under short and narrow shading conditions, as mentioned in Table 6.

3.5 Ladder (LD) PV Array Configuration

The PV modules within the first three columns of each row are linked together in a parallel arrangement. Subsequently, the rows themselves are connected in a series configuration. The MATLAB simulation connection and the simulated I-V and P-V curves are shown in Figs. 14 and 15.

The number of local peaks generated is 3, 2, 2, 4, and 2 under DIA, SN, SW, LN, and LW shading conditions, respectively, with the global peak of 29.4 VpeIpe produced by the LD configuration under the diagonal shading condition, as mentioned in Table 7.

3.6 Triple Cross Tied (TrCT) PV Array Configuration

The arrangement of interconnection in the TrCT configuration draws inspiration from the structure of staircase flights and represents a modified version of the BL or HC configurations. In this arrangement, a sequence of three modules is interconnected, followed by a subsequent gap. Additionally, it can be interpreted as a cross-tie configuration due to the inclusion of cross ties that establish connections among the parallel strings. The MATLAB simulation connection is shown in Figure 16, and the simulated I-V and P-V curves are presented in Figure 17.

The number of local peaks generated is 5, 2, 2, 4, and 2 under DIA, SN, SW, LN, and LW shading conditions, respectively, with the global peak of 31.8 VpeIpe produced by the TrCT configuration under diagonal shading condition, as mentioned in Table 8.

3.7 Series Parallel - Total Cross Tied (SPTCT) PV Array Configuration

The SPTCT arrangement is formulated by integrating the S-P and T-C-T configurations in series. Consequently, a uniform current traverses both the SP and TCT configurations. Notably, the S-P-T-C-T topology exhibits enhanced performance compared to the SP, BL, and HC topologies across a wide spectrum of shading scenarios. The connection scheme for MATLAB simulations is presented in Figure 18, and the corresponding simulated I-V and P-V curves are shown in Figure 19.

The number of local peaks generated is 4, 2, 2, 4 and 2 under DIA, SN, SW, LN, and LW shading conditions, respectively, with the global peak of 28.8 VpeIpe produced by the SPTCT configuration under short and narrow shading conditions, as mentioned in Table 9.
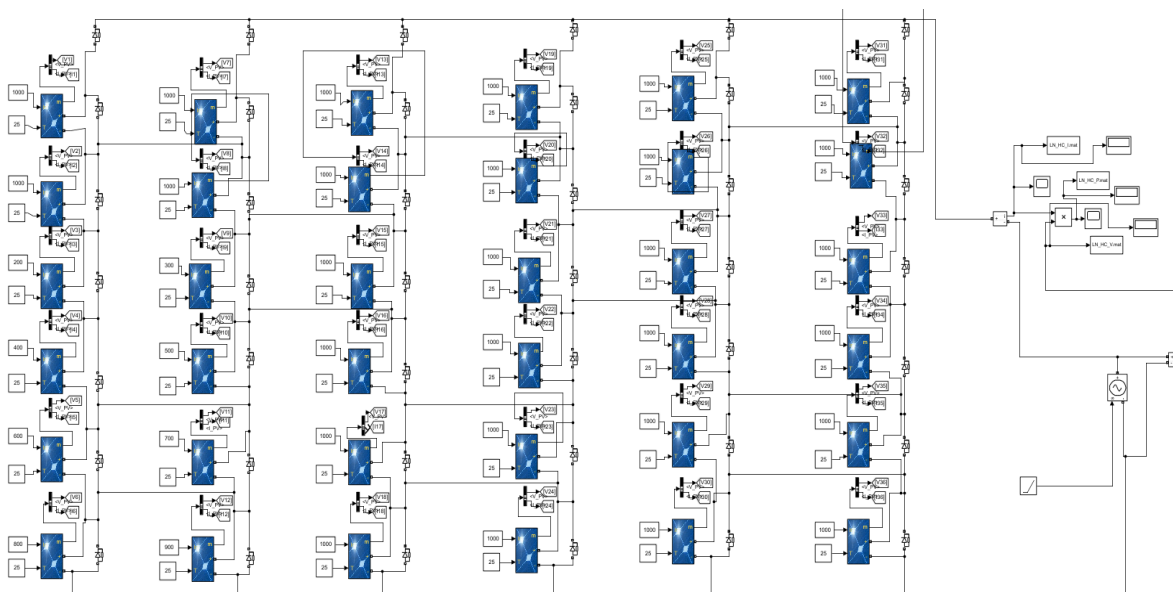
Figure 12. Simulink® connection diagram for the configuration of the HC PV array

Table 6. Representation of PV array parameters for HC Configuration under various shading conditions

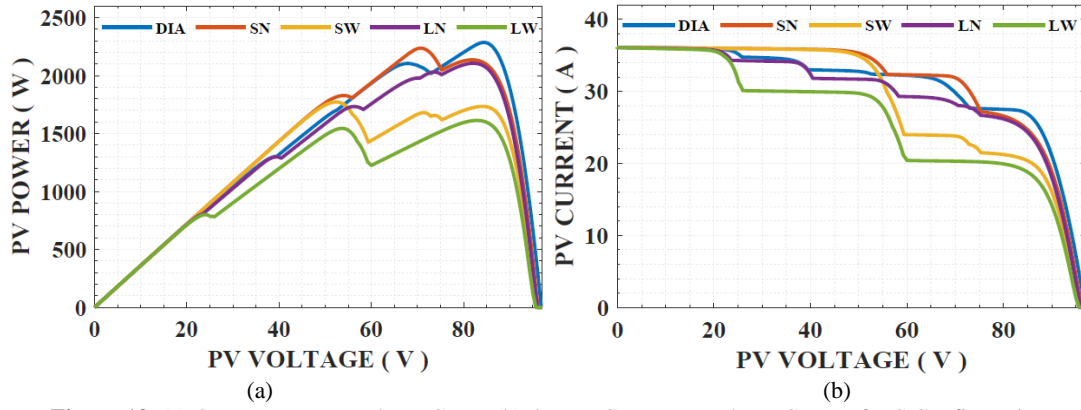| Shading Scheme	Interval at which Array Voltage, Current and Power change				
DIA	$0 \leq V_{Te} \leq 2V_{pe}$	$2\,V_{pe} \leq V_{Te} \leq 3\,V_{pe}$	$3\,V_{pe} \leq V_{Te} \leq 4\,V_{pe}$	$4\,V_{pe} \leq V_{Te} \leq 5\,V_{pe}$	$5\,V_{pe} \leq V_{Te} \leq 6\,V_{pe}$
Working modules	2-6,10-12,16-18,20,21,23,24,25-28,31-34	2,3,4,11,12,17,18,20, 21,25-28,30,31-34,36	2-4,9,15,19,25, 26,31-34	2-4,8,13,19, 25-26,31	1,7,14,22,29,35
V_{Te}	$2\,V_{pe}$	$3\,V_{pe}$	$4\,V_{pe}$	$5\,V_{pe}$	$6\,V_{pe}$
I_{Te}	$6\,I_{pe}$	$5.8\,I_{pe}$	$5.5\,I_{pe}$	$5.4\,I_{pe}$	$4.6\,I_{pe}$
P_{Te}	$12\,V_{pe}I_{pe}$	$17.4\,V_{pe}I_{pe}$	$22\,V_{pe}I_{pe}$	$27\,V_{pe}I_{pe}$	**$27.6\,V_{pe}I_{pe}$**
SN	$0 \leq V_{Te} \leq 4V_{Pe}$			$4V_{Pe} \leq V_{Te} \leq 5V_{Pe}$	$5V_{Pe} \leq V_{Te} \leq 6V_{Pe}$
Working modules	1-4,7-10,13-36			6,12,16-18,20-24,25-36	5,11, 16-18,20-24,25-36
V_{Te}	$4\,V_{Pe}$			$5\,V_{Pe}$	$6\,V_{Pe}$
I_{Te}	$6\,I_{Pe}$			$5.6\,I_{Pe}$	$4.6\,I_{Pe}$
P_{Te}	$24\,V_{Pe}I_{Pe}$			**$28\,V_{Pe}I_{Pe}$**	$27.6\,V_{Pe}I_{Pe}$
SW	$0 \leq V_{Te} \leq 4V_{Pe}$			$4V_{Pe} \leq V_{Te} \leq 5V_{Pe}$	$5V_{Pe} \leq V_{Te} \leq 6V_{Pe}$
Working modules	1-4,7-10,13-16,19-22,25-36			5,11,17,23,28-30,32-36	6,12,18,24,28-30,32-36
V_{Te}	$4\,V_{Pe}$			$5\,V_{Pe}$	$6\,V_{Pe}$
I_{Te}	$6\,I_{Pe}$			$4.1\,I_{Pe}$	$3.7\,I_{Pe}$
P_{Te}	**$24\,V_{Pe}I_{Pe}$**			$20.5\,V_{Pe}I_{Pe}$	$22.2\,V_{Pe}I_{Pe}$
LN	$0 \leq V_{Te} \leq 2V_{Pe}$	$2V_{Pe} \leq V_{Te} \leq 3V_{Pe}$	$3V_{Pe} \leq V_{Te} \leq 4V_{Pe}$	$4V_{Pe} \leq V_{Te} \leq 5V_{Pe}$	$5V_{Pe} \leq V_{Te} \leq 6V_{Pe}$
Working modules	1,2,7,8,13,14,19-22,25-36	6,12,16-36	5,11,16-18,20-36	4,10,16-18,20-36	3,9,15,20-36
V_{Te}	$2V_{Pe}$	$3\,V_{Pe}$	$4\,V_{Pe}$	$5\,V_{Pe}$	$6\,V_{Pe}$
I_{Te}	$6\,I_{Pe}$	$5.8\,I_{Pe}$	$5.4\,I_{Pe}$	$5\,I_{Pe}$	$4.6\,I_{Pe}$
P_{Te}	$12\,V_{Pe}I_{Pe}$	$17.4\,V_{Pe}I_{Pe}$	$21.6\,V_{Pe}I_{Pe}$	$25\,V_{Pe}I_{Pe}$	**$27.6\,V_{Pe}I_{Pe}$**
LW	$0 \leq V_T \leq 2V_P$	$2V_P \leq V_T \leq 3V_P$ $3V_P \leq V_T \leq 4V_P$		$4V_P \leq V_T \leq 6V_P$	
Working modules	1,2,7,8,13,14,19,20,25,26,31-34	4,6,10,12,16,18,22,24,28-30,32-36		3,5,9,11,15,17,21,23,27,28,35,36	
V_{Te}	$2V_{Pe}$	$4\,V_{Pe}$		$6\,V_{Pe}$	
I_{Te}	$6\,I_{Pe}$	$5\,I_{Pe}$		$3.4\,I_{Pe}$	
P_{Te}	$12\,V_{Pe}I_{Pe}$	$20\,V_{Pe}I_{Pe}$		**$20.4\,V_{Pe}I_{Pe}$**	

Figure 13. (a) Output Power - Voltage Curve (b) Output Current - Voltage Curve of HC Configuration

Figure 14. Simulink® connection diagram for the configuration of the LD PV array

Table 7 Representation of PV array parameters for LD Configuration under various shading conditions

Shading Scheme	Interval at which Array Voltage, Current and Power change				
DIA	$0 \leq V_{Te} \leq 3 \ V_{Pe}$		$3V_{Pe} \leq V_{Te} \leq 4V_{Pe}$	$4V_{Pe} \leq V_{Te} \leq 5V_{Pe}$	$5V_{Pe} \leq V_{Te} \leq 6V_{Pe}$
Working modules	4-6,10-12,16-18,19-21,25-27,31-33		3,9,15,24,30,36	2,8,14,23,29,35	1,7,13,22,28,34
V_{Te}	3 V_{Pe}		4 V_{Pe}	5 V_{Pe}	6 V_{Pe}
I_{Te}	6 V_{Pe}		5.3 I_{Pe}	5.1 I_{Pe}	4.9 I_{Pe}
P_{Te}	18 $V_{Pe} I_{Pe}$		21.2 $V_{Pe} I_{Pe}$	25.5 $V_{Pe} I_{Pe}$	**29.4 $V_{Pe} I_{Pe}$**
SN	$0 \leq V_{Te} \leq 4V_{Pe}$			$4V_{Pe} \leq V_{Te} \leq 5V_{Pe}$	$5V_{Pe} \leq V_{Te} \leq 6V_{Pe}$
Working modules	1-4,7-10,13-16,25-36			6,12,18,25-36	5,11,17,25-36
V_{Te}	4 V_{Pe}			5 V_{Pe}	6 V_{Pe}
I_{Te}	6 I_{Pe}			5.6 I_{Pe}	4.6 I_{Pe}
P_{Te}	24 $V_{Pe} I_{Pe}$			**28 $V_{Pe} I_{Pe}$**	27.6 $V_{Pe} I_{Pe}$
SW	$0 \leq V_{Te} \leq 4V_{Pe}$			$4V_{Pe} \leq V_{Te} \leq 5V_{Pe}$	$5V_{Pe} \leq V_{Te} \leq 6V_{Pe}$
Working modules	1-4,7-10,13-16,19-22,25-28,31-34			5,11,17,23,29,35	6,12,18,24,30,36,
V_{Te}	4 V_{Pe}			5 V_{Pe}	6 V_{Pe}
I_{Te}	6 I_{Pe}			4 I_{Pe}	3.7 I_P
P_{Te}	**24 $V_{Pe} I_{Pe}$**			20 $V_{Pe} I_{Pe}$	22.2 $V_{Pe} I_{Pe}$
LN	$0 \leq V_{Te} \leq 2V_{Pe}$	$2V_{Pe} \leq V_{Te} \leq 3V_{Pe}$	$3V_{Pe} \leq V_{Te} \leq 4V_{Pe}$	$4V_{Pe} \leq V_{Te} \leq 5V_{Pe}$	$5V_{Pe} \leq V_{Te} \leq 6V_{Pe}$
Working modules	1,2,7,8,13,14,19-36	6,12,18,19-36	5,11,17,19-36	4,10,16,19-36	3,9,5,19-36
V_{Te}	2V_{Pe}	3 V_{Pe}	4 V_{Pe}	5 V_{Pe}	6 V_{Pe}
I_{Te}	6 I_{Pe}	5.8 I_{Pe}	5.4 I_{Pe}	5 I_{Pe}	4.5 I_{Pe}

Shading Scheme	Interval at which Array Voltage, Current and Power change				
P$_{Te}$	12 V$_{Pe}$I$_{Pe}$	17.4 V$_{Pe}$I$_{Pe}$	21.6 V$_{Pe}$I$_{Pe}$	25 V$_{Pe}$I$_{Pe}$	**27 V$_{Pe}$I$_{Pe}$**
LW	$0 \leq V_{Te} \leq V_{Pe}$	$2V_{Pe} \leq V_{Te} \leq 4V_{Pe}$		$4V_{Pe} \leq V_{Te} \leq 6V_{Pe}$	
Working modules	1,2,7,8,13,14,19,20,25,26,31,32	4,6,10,12,16,18,22,24,28,30,34,36		3,5,9,11,15,17,21,23,27,29,33,35	
V$_{Te}$	2V$_{Pe}$	4 V$_{Pe}$		6 V$_{Pe}$	
I$_{Te}$	6 I$_{Pe}$	5 I$_{Pe}$		3.5 I$_{Pe}$	
P$_{Te}$	12 V$_{Pe}$I$_{Pe}$	20 V$_{Pe}$I$_{Pe}$		**21 V$_{Pe}$I$_{Pe}$**	

Figure 15. (a) Output Power - Voltage Curve (b) Output Current - Voltage Curve of LD Configuration
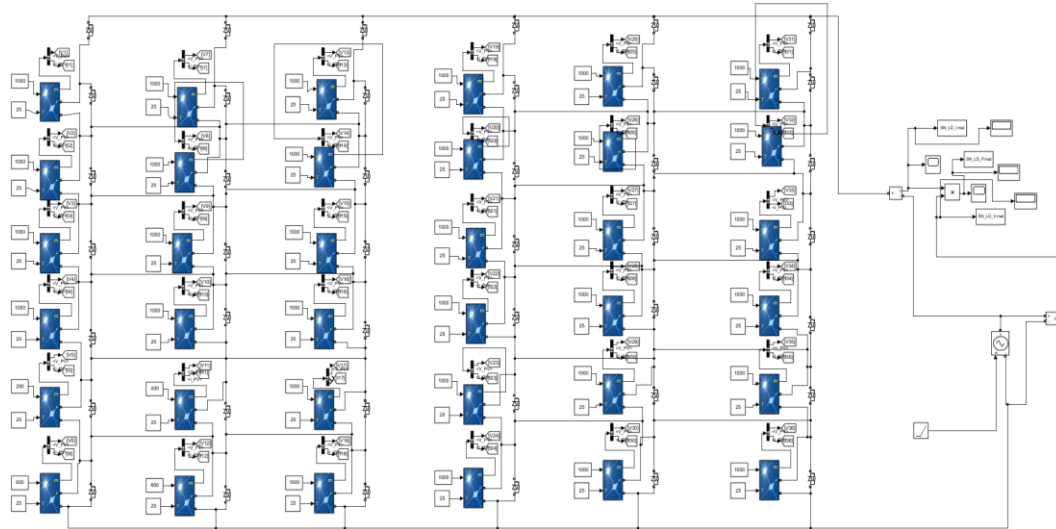

Figure 16. Simulink® connection diagram for the configuration of the TrCT PV array

Table 8. Representation of PV array parameters for TrCT Configuration under various shading conditions

Shading Scheme	Interval at which Array Voltage, Current and Power change					
DIA	$0 \leq V_{Te} \leq V_{Pe}$	$V_{Pe} \leq V_{Te} \leq 2V_{Pe}$	$2V_{Pe} \leq V_{Te} \leq 3V_{Pe}$	$3V_{Pe} \leq V_{Te} \leq 4V_{Pe}$	$4V_{Pe} \leq V_{Te} \leq 5V_{Pe}$	$5V_{Pe} \leq V_{Te} \leq 6V_{Pe}$
Working modules	3-6,10,12,17,18, 24,30,36	4-6,10,12,16-18,21,24,27,29,30,34-36	4-6,10-12,15-16,20,22,26-28,31-35	2,8,9,13-15,19-21,25-28,31-35	2,8,13,14,19-21,25-28,31-35	1,7,13,14,19-21,25-28,31-34
V$_{Te}$	V$_{pe}$	2 V$_{pe}$	3 V$_{pe}$	4 V$_{pe}$	5 V$_{pe}$	6 V$_{pe}$
I$_{Te}$	5.8 I$_{pe}$	5.7 I$_{pe}$	5.6 I$_{pe}$	5.5 I$_{pe}$	5.4 I$_{pe}$	5.3 I$_{pe}$

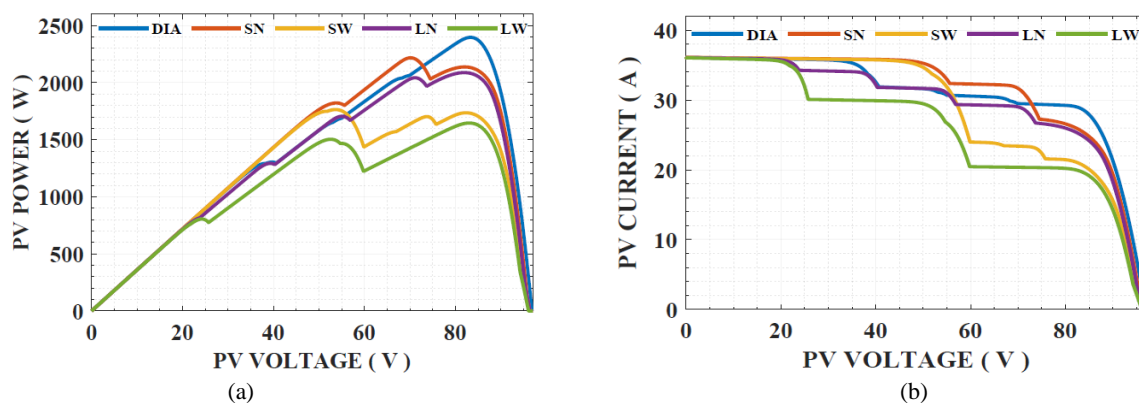| Shading Scheme	Interval at which Array Voltage, Current and Power change					
P_{Te}	5.8 $V_{pe} I_{pe}$	11.4 $V_{pe} I_{pe}$	16.8 $V_{pe} I_{pe}$	22 $V_{pe} I_{pe}$	27 $V_{pe} I_{pe}$	**31.8 $V_{pe} I_{pe}$**
SN	$0 \leq V_{Te} \leq 4V_{Pe}$				$4V_{Pe} \leq V_{Te} \leq 5V_{Pe}$	$5V_{Pe} \leq V_{Te} \leq 6V_{Pe}$
Working modules	1-4,7-10,13-17,19-36				6,12,16-18,22-24,27-30,33-36	5,11,16,17,22-24,27-30,33-36
V_{Te}	4 V_{Pe}				5 V_{Pe}	6 V_{Pe}
I_{Te}	6 I_{Pe}				5.7 I_{Pe}	4.7 I_{Pe}
P_{Te}	24 $V_{Pe} I_{Pe}$				**28.5 $V_{Pe} I_{Pe}$**	28.2 $V_{Pe} I_{Pe}$
SW	$0 \leq V_{Te} \leq 4V_{Pe}$				$4V_{Pe} \leq V_{Te} \leq 5V_{Pe}$	$5V_{Pe} \leq V_{Te} \leq 6V_{Pe}$
Working modules	1-4,7-10,13-16,19-22,25-28,31-35				5,11,17,23,29,34,35	6,12,18,24,30,36
V_{Te}	4 V_{Pe}				5 V_{Pe}	6 V_{Pe}
I_{Te}	6 I_{Pe}				4 I_{Pe}	3.7 I_{Pe}
P_{Te}	**24 $V_{Pe} I_{Pe}$**				20 $V_{Pe} I_{Pe}$	22.2 $V_{Pe} I_{Pe}$
LN	$0 \leq V_{Te} \leq 2V_{Pe}$		$2V_{Pe} \leq V_{Te} \leq 3V_{Pe}$	$3V_{Pe} \leq V_{Te} \leq 4V_{Pe}$	$4V_{Pe} \leq V_{Te} \leq 5V_{Pe}$	$5V_{Pe} \leq V_{Te} \leq 6V_{Pe}$
Working modules	1,2,7,8,13,14,19-21,25-28,31-35		6,12,18,20,21,23,24,26-36	5,11,16,20-24,26-36	4,10,16,17,20-24,26-36	3,9,15,20,21,26-28,33-36
V_{Te}	2 V_{Pe}		3 V_{Pe}	4 V_{Pe}	5 V_{Pe}	6 V_{Pe}
I_{Te}	6 I_{Pe}		5.7 I_{Pe}	5.5 I_{Pe}	5 I_{Pe}	4.6 I_{Pe}
P_{Te}	12 $V_{Pe} I_{Pe}$		17.2 $V_{Pe} I_{Pe}$	22 $V_{Pe} I_{Pe}$	25 $V_{Pe} I_{Pe}$	**27.6 $V_{Pe} I_{Pe}$**
LW	$0 \leq V_T \leq 2V_P$		$2V_P \leq V_T \leq 4V_P$		$4V_P \leq V_T \leq 6V_P$	
Working modules	1,2,7,8,13,14,19,20,25,26,31,32		4,6,10,12,16,18,22,2428,30,34,36		3,5,9,11,15,17,21,23,27-29,33-36	
V_{Te}	2 V_{Pe}		4 V_{Pe}		6 V_{Pe}	
I_{Te}	6 I_{Pe}		5.1 I_{Pe}		3.5 I_{Pe}	
P_{Te}	12 $V_{Pe} I_{Pe}$		20.4 $V_{Pe} I_{Pe}$		**21 $V_{Pe} I_{Pe}$**	

Figure 17 (a) Output Power - Voltage Curve (b) Output Current - Voltage Curve of TrCT Configuration
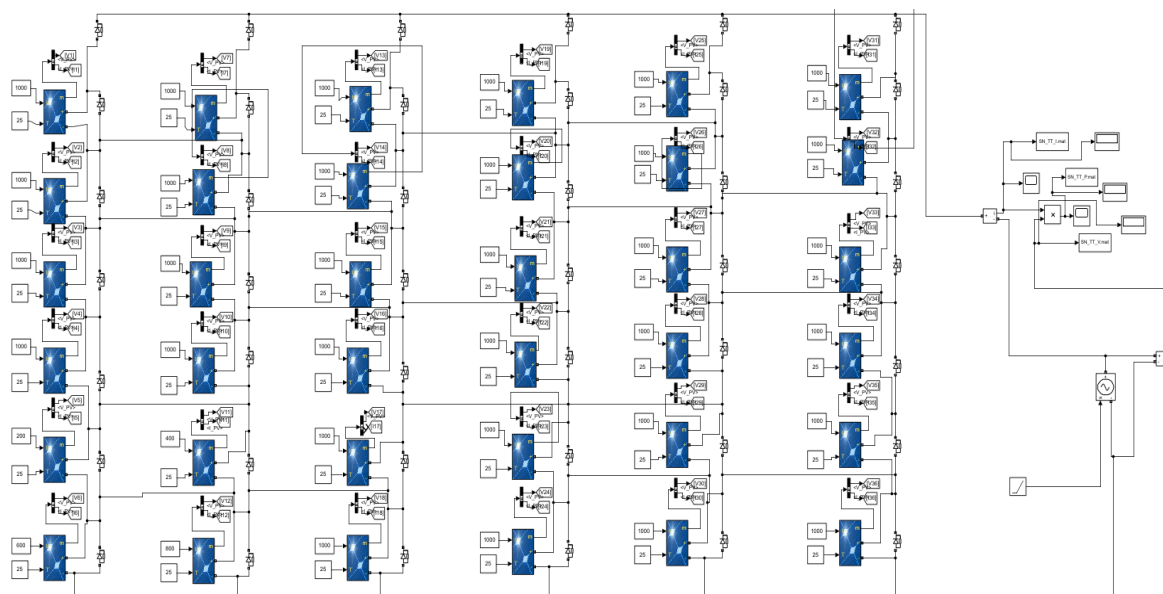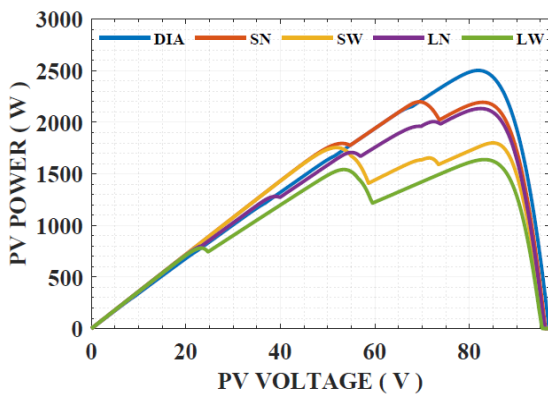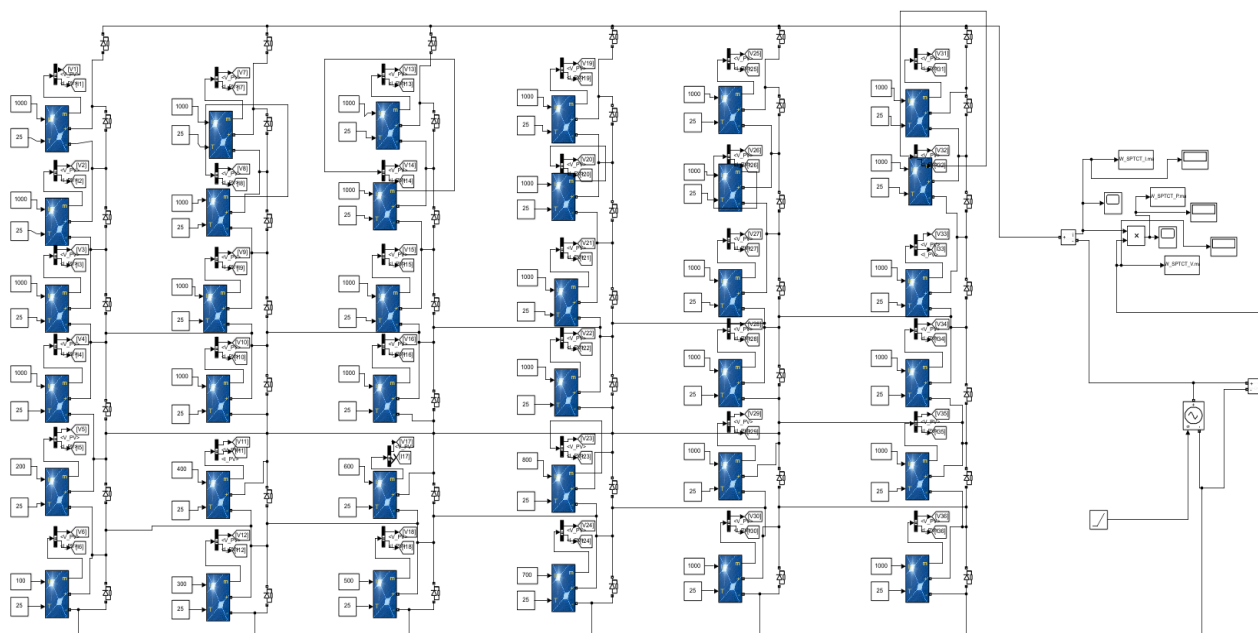
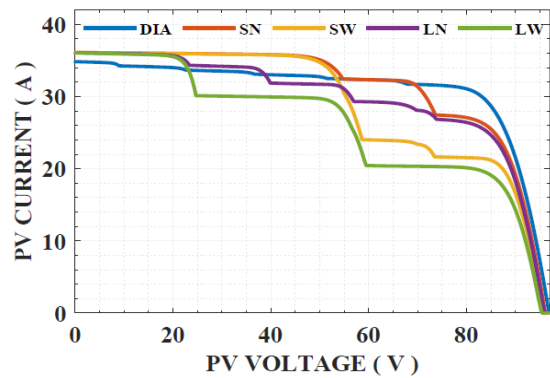**Figure 18** Simulink® connection diagram for the configuration of the SPTCT PV array

Table 9. Representation of PV array parameters for SPTCT Configuration under various shading conditions

Shading Scheme	Interval at which Array Voltage, Current and Power change				
Diagonal	$0 \leq V_{Te} \leq 2V_{Pe}$	$2V_{Pe} \leq V_{Te} \leq 3V_{Pe}$	$3V_{Pe} \leq V_{Te} \leq 4V_{Pe}$	$4V_{Pe} \leq V_{Te} \leq 5V_{Pe}$	$5V_{Pe} \leq V_{Te} \leq 6V_{Pe}$
Working Panels	7,13,19,25,31, 2,14,20,26,32, 3,9,21,27,33	19,25,31,20,26,32,21,27,33,6,12,18,24,30,36	19,25,31,20,26,32,21,27,33,5,11,17,23,29,35	19,25,31,20,26,32,21,27,33,4,10,16,22,28,34	1,7,13,19,25,31 2,8,14,20,26,32 3,9,15,21,27,33
V_{Te}	$2V_{Pe}$	$3 V_{Pe}$	$4 V_{Pe}$	$5 V_{Pe}$	$6 V_{Pe}$
I_{Te}	$6 I_{Pe}$	$5.8 I_{Pe}$	$5.7 I_{Pe}$	$5.6 I_{Pe}$	$4.2 I_{Pe}$
P_{Te}	$12 V_{Pe} I_{Pe}$	$17.4 V_{Pe} I_{Pe}$	$22.8 V_{Pe} I_{Pe}$	**$28 V_{Pe} I_{Pe}$**	$25.2 V_{Pe} I_{Pe}$
SN	$0 \leq V_{Te} \leq 4V_{Pe}$			$4V_{Pe} \leq V_{Te} \leq 5V_{Pe}$	$5V_{Pe} \leq V_{Te} \leq 6V_{Pe}$
Working modules	1-4,7-10,13-16,19-22,25-28,31-35			6,12,18,24,30, 36	5,11,17,23,29, 35
V_{Te}	$4 V_{Pe}$			$5 V_{Pe}$	$6 V_{Pe}$
I_{Te}	$6 I_{Pe}$			$5.6 I_{Pe}$	$4.8 I_{Pe}$
P_{Te}	$24 V_{Pe} I_{Pe}$			$28 V_{Pe} I_{Pe}$	**$28.8 V_{Pe} I_{Pe}$**
SW	$0 \leq V_{Te} \leq 4V_{Pe}$			$4V_{Pe} \leq V_{Te} \leq 5V_{Pe}$	$5V_{Pe} \leq V_{Te} \leq 6V_{Pe}$
Working modules	1-4,7-10,13-16,19-22,25-28,31-35			5,11,17,23,29, 35	6,12,18,24,30, 36
V_{Te}	$4 V_{Pe}$			$5 V_{Pe}$	$6 V_{Pe}$
I_{Te}	$6 I_{Pe}$			$4.1 I_{Pe}$	$3.7 I_{Pe}$
P_{Te}	**$24 V_{Pe} I_{Pe}$**			$20.4 V_{Pe} I_{Pe}$	$22.2 V_{Pe} I_{Pe}$
LN	$0 \leq V_{Te} \leq 2V_{Pe}$	$2V_{Pe} \leq V_{Te} \leq 3V_{Pe}$	$3V_{Pe} \leq V_{Te} \leq 4V_{Pe}$	$4V_{Pe} \leq V_{Te} \leq 5V_{Pe}$	$5V_{Pe} \leq V_{Te} \leq 6V_{Pe}$
Working modules	1,2,7,8,13-15,19-21,25-27,31-33	6,12,18,24,30, 36	5,11,17,23,29,35	4,10,16,22,28, 34	3,9,15,21,27,33
V_{Te}	$2V_{Pe}$	$3 V_{Pe}$	$4 V_{Pe}$	$5 V_{Pe}$	$6 V_{Pe}$
I_{Te}	$6 I_{Pe}$	$5.8 I_{Pe}$	$5.4 I_{Pe}$	$5 I_{Pe}$	$4.6 I_{Pe}$
P_{Te}	$12 V_{Pe} I_{Pe}$	$17.4 V_{Pe} I_{Pe}$	$21.6 V_{Pe} I_{Pe}$	$25 V_{Pe} I_{Pe}$	**$27.6 V_{Pe} I_{Pe}$**
LW	$0 \leq V_{Te} \leq 2V_{Pe}$	$2V_{Pe} \leq V_{Te} \leq 4V_{Pe}$		$4V_{Pe} \leq V_{Te} \leq 6V_{Pe}$	
Working modules	1,2,7,8,13,14,19,20,25-27,31-33	4,6,10,12,16,18,22,24,28,30,34,36		3,9,15,21,27,33	
V_{Te}	$2V_{Pe}$	$4 V_{Pe}$		$6 V_{Pe}$	
I_{Te}	$6 I_{Pe}$	$5.1 I_{Pe}$		$3.5 I_{Pe}$	
P_{Te}	$12 V_{Pe} I_{Pe}$	$20.4 V_{Pe} I_{Pe}$		**$21 V_{Pe} I_{Pe}$**	

(a)   (b)

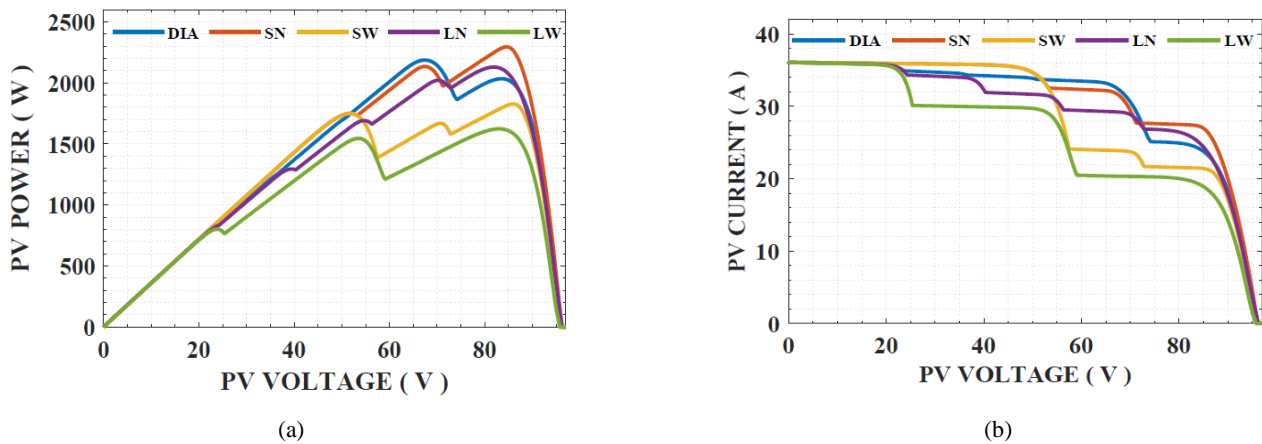**Figure 19.** (a) Output Power - Voltage Curve (b) Output Current - Voltage Curve of SPTCT Configuration

3.8 Bridge Link - Total Cross Tied (BLTCT) PV Array Configuration

This configuration is structured by establishing a series connection between the B-L and T-C-T topologies, ensuring a uniform current distribution across both the B-L and T-C-T configurations. Notably, the B-L-T-C-T topology excels in performance compared to the S-P, B-L, and H-C topologies. The connection scheme for MATLAB simulations is presented in Figure 20, and the corresponding simulated I-V and P-V curves are shown in Figure 21.

The number of local peaks generated is 5, 2, 2, 4 and 2 under DIA, SN, SW, LN, and LW shading conditions, respectively, with the global peak of 31.8 VpeIpe produced by the BLTCT configuration under diagonal shading conditions, as mentioned in Table 10.

3.9 Honey Comb - Total Cross Tied (HCTCT) PV Array Configuration

This configuration is structured by establishing a series connection between the H-C and T-C-T topologies, ensuring a uniform current distribution across both the H-C and T-C-T configurations. Notably, the H-C-T-C-T topology excels in performance compared to the S-P, B-L, and T-C-T topologies. The connection scheme for MATLAB simulations is presented in Figure 22, and the corresponding simulated I-V and P-V curves are shown in Figure 23.

The number of local peaks generated is 5, 2, 2, 4, and 2 under DIA, SN, SW, LN, and LW shading conditions, respectively, with the global peak of 31.8 VpeIpe produced by the BLTCT configuration under diagonal shading conditions, as mentioned in Table 11.

4. RESULTS AND DISCUSSION

This section outlines the results derived from assessing both conventional and hybrid photovoltaic (PV) array topologies across diverse shading patterns elaborated upon in Section 3. The parameters provided in reference (Suresh 2022) are employed to assess the performance of all PV arrangements across varying shading conditions, as indicated in Tables 12 and 13, and comparative assessment is shown in Figure 23.

4.1 Under No Shading Condition

Each PV module within the array configurations is exposed to solar irradiance of 1000 W/m2. Under this shading scenario, both the conventional and proposed hybrid topologies operate

at Voc and Isc values of 97.2 V and 36.14 A, respectively. A singular peak at 2746 W is observed in the P-V characteristics with the corresponding values for voltage (Vpe) and current (Ipe) are 81 V and 33.87 A and the FF & η are 0.782 and 14.12%, respectively.

4.2 Under Diagonal (DIA) Shading Condition

The TCT configuration produces the highest global peak power of 2490 W. The associated values for voltage (Vpe) and current (Ipe) are 84.7 V and 28.3 A, respectively. Comparatively, the SP, BL, HC, LD, TrCT, SPTCT, BLTCT, and HCTCT arrangements result in 1, 1, 4, 3, 5, 4, 5, and 5 local peaks, respectively. For the TCT arrangement, PL, η, and fill factor (FF) are 1.88%, 13.84%, and 0.68, as specified in Table 13.

4.3 Under Short Narrow (SN) Shading Condition

The TCT configuration produces the highest global peak power of 2296 W. The associated values for voltage (Vpe) and current (Ipe) are 84.5 V and 27.17 A, respectively. Comparatively, the SP, BL, HC, LD, TrCT, SPTCT, BLTCT, and HCTCT arrangements result in 2 local peaks, respectively. For the TCT arrangement, the PL, η, and fill factor (FF) are 11.42 %, 12.57 %, and 0.68, as specified in Table 13.

4.4 Under Short Wide (SW) Shading Condition

The TCT configuration produces the highest global peak power of 1828 W. The associated values for voltage (Vpe) and current (Ipe) are 86.1 V and 21.23 A, respectively. Comparatively, the SP, BL, HC, LD, TrCT, SPTCT, BLTCT, and HCTCT arrangements result in 2 local peaks, respectively. For the TCT arrangement, the PL, η, and fill factor (FF) are 24.15 %, 10.74 %, and 0.54, as specified in Table 13.

4.5 Under Long Narrow (LN) Shading Condition

The TCT configuration produces the highest global peak power of 2224 W. The associated values for voltage (Vpe) and current (Ipe) are 84 V and 26.45 A, respectively. Comparatively, the SP, BL, HC, LD, TrCT, SPTCT, BLTCT, and HCTCT arrangements result in 4 local peaks respectively. For the TCT arrangement, the PL, η, and fill factor (FF) are 9.89 %, 12.79 %, and 0.65, as specified in Table 13.

4.6 Under Long Wide (LW) Shading Condition

The TCT configuration produces the highest global peak power of 1687 W. The associated values for voltage (Vpe) and

current (Ipe) are 85 V and 19.85 A, respectively. Comparatively, the SP, BL, HC, LD, TrCT, SPTCT, BLTCT, and HCTCT arrangements result in 2 local peaks, respectively.

For the TCT arrangement, PL, η, and fill factor (FF) are 22.97 %, 11.57 %, and 0.49, as specified in Table 13.

Table 12 Global Powers, local Powers, Open circuit voltage and short circuit current of Conventional and Hybrid PV configurations

Topology	Voc (V)	Isc (A)	Global Values			Local Values		
			P_{pe} (W)	V_{pe} (V)	I_{pe} (A)	P_{pe} (W)	V_{pe} (V)	I_{pe} (A)
No Shading Condition								
For all patterns	97.2	36.14	2746	81	33.87	--	--	---
Diagonal (DIA)								
SP	96.4	36.11	2234	65.75	33.95	1665	86.93	19.1
TCT	96.4	36.11	**2490**	84.7	28.3	221	6.4	34.5
						672	19.8	33.9
						1135	34	33.3
						1599	49	32.64
						2033	63.4	32
BL	95.9	36.12	2233	66.1	33.82	1689	86.6	19.55
HC	96.84	36.14	2286	84.55	27.15	848	23.85	35.58
						1278	37.55	34.1
						1683	51.61	32.61
						2105	68.1	30.93
LD	96.85	36.14	2396	83.98	28.6	1305	39.76	32.86
						1668	53.67	31.11
						2039	67.91	30.1
TrCT	96.8	34.89	2478	81.8	30.6	310	9	34.26
						775	23	33.66
						1235	37.3	33.08
						1700	52.4	32.5
						2145	67.3	31.8
SPTCT	95.36	36.2	2188	67.069	32.42	795	22.55	35.1
						1261	36.46	34.34
						1703	50.06	33.83
						2035	82.63	24.48
BLTCT	95.36	36.2	2481	80.39	30.69	231	6.61	34.48
						683	20.1	33.88
						1149	34.32	33.26
						1631	49.48	32.76
						2107	65.71	31.87
HCTCT	95.36	36.2	2308	82.41	27.82	325	9.14	35.36
						744	21.44	34.56
						1229	36.1	33.86
						1699	51.1	33.14
						2104	68.24	30.64
Short Narrow (SN)								
SP	96.4	36.11	2257	72.18	31.32	1865	54.88	34.03
						2101	81.6	25.72
TCT	96.4	36.11	**2296**	84.5	27.17	1749	51.4	34
						2135	67.4	31.66
BL	96.4	36.11	2216	70	31.67	1816	53.7	33.82
						2160	82	26.34
HC	96.4	36.11	2236	70.6	31.66	1826	53.52	34.14
						2136	82	26
LD	96.84	36.13	2218	70	31.67	1822	53.6	34
						2137	82	26.08
TrCT	96.86	34.89	2198	69.3	31.7	1794	52.7	34
						2193	81	26.9
SPTCT	95.35	36.1	2295	84.7	27.08	1749	51.4	34
						2135	67.3	31.72
BLTCT	95.35	36.1	2295	84.72	27.09	1748	51.2	34.09
						2135	67.42	31.66
HCTCT	95.35	36.1	2294	84.85	27.05	1749	51.56	33.86
						2134	67.72	31.5
Short Wide (SW)								
SP	96.4	36.11	1791	53	33.74	1664	72	23.15
						1685	83.5	20.19

Topology	Voc (V)	Isc (A)	Global Values			Local Values		
			P_{pe} (W)	V_{pe} (V)	I_{pe} (A)	P_{pe} (W)	V_{pe} (V)	I_{pe} (A)
TCT	96.4	36.11	**1828**	86.1	21.23	1749	52	33.68
						1668	70.8	23.54
BL	96.4	36.11	1771	84.55	20.96	1767	52.47	33.66
						1659	71.8	23.11
HC	96.4	36.11	1772	52.46	33.79	1679	71.5	23.48
						1734	84.2	20.59
LD	96.84	36.13	1764	53.6	32.91	1702	73.7	23.1
						1735	82.8	20.94
TrCT	96.86	34.89	1800	85	21.18	1755	52	33.69
						1654	71.5	23.1
SPTCT	95.35	36.1	1827	86.22	21.2	1749	51.5	33.94
						1667	70.9	23.52
BLTCT	95.35	36.1	1827	86.22	21.21	1749	51.63	33.93
						1668	70.81	23.53
HCTCT	95.35	36.1	1827	86.29	21.18	1749	51.93	33.66
						1667	71	23.49
Long Narrow (LN)								
SP	96.4	36.11	2092	73.3	28.55	845	24.43	34.6
						1323	39.73	33.2
						1751	57	30.7
						2050	81.76	25.1
TCT	96.4	36.11	**2224**	84	26.45	736	20.84	35.34
						1227	36.63	33.5
						1630	52.3	31.15
						1962	68	28.82
BL	96.4	36.11	2098	82	25.56	792	22.38	35.57
						1304	39.5	33
						1730	56.1	30.83
						2022	73.16	27.62
HC	96.4	36.11	2106	82	25.64	793	22.61	35.03
						1297	39	33.21
						1733	56	30.94
						2030	73.6	27.6
LD	96.84	36.13	2088	82	25.46	796	22.6	35.17
						1292	39.33	32.86
						1705	55	30.96
						2043	71	28.77
TrCT	96.86	34.89	2133	82	26	790	22.6	34.95
						1279	39.35	32.5
						1707	55	31.1
						2006	72	27.81
SPTCT	95.35	36.1	2130	82	25.86	814	23.2	35
						1295	39.3	32.92
						1691	54.8	30.88
						2021	70.35	28.75
BLTCT	95.35	36.1	2157	83.13	25.84	785	22.42	35.08
						1266	38.4	32.96
						1661	53.6	31
						2003	69.9	28.63
HCTCT	95.35	36.1	2130	82	25.97	810	23	35.17
						1294	39.1	33
						1691	54.73	30.92
						2021	70.21	28.79
Long Wide (LW)								
SP	96.4	36.11	1586	82.84	19.14	796	23	34.36
						1560	54.28	28.78
TCT	96.4	36.11	**1687**	85	19.85	779	23	33.85
						1525	52.8	28.9
BL	96.4	36.11	1607	82.75	19.4	797	23.7	33.6
						1556	53.9	28.86
HC	96.4	36.11	1612	83.2	19.39	795	23.33	34
						1543	53.3	28.8
LD	96.84	36.13	1646	83.3	19.8	805	24.29	33.15
						1504	52.6	28.57

| Topology	Voc (V)	Isc (A)	Global Values			Local Values		
			P_{pe} (W)	V_{pe} (V)	I_{pe} (A)	P_{pe} (W)	V_{pe} (V)	I_{pe} (A)
TrCT	96.86	34.89	1638	83.5	19.6	780	22.93	33.98
						1542	53.3	28.89
SPTCT	95.35	36.1	1624	83.1	19.54	800	23.61	33.86
						1545	53.74	28.76
BLTCT	95.35	36.1	1658	83.88	19.77	785	23.17	33.98
						1532	53.22	28.73
HCTCT	95.35	36.1	1624	82.9	19.58	801	23.69	33.9
						1545	53.74	28.81

Table 13. % Mismatch Power Loss, Shading Loss, Mis-leading Loss, Fill Factor, and Efficiency of Conventional and Hybrid PV configurations

| Topology	Sum of Peak Powers under shading condition (W)	NO shading Array Maximum Power (W)	Shading Loss (W)	% Mismatch Loss (P_L)	Mis-leading Loss	Fill Factor (FF)	Input Insolation (P_{in}) = Insolation *area	Efficiency (η) = P_{mpp}/ P_{in}
No Shading Condition								
For all configurations	2746.08	2745	---	---	----	0.782	19440	14.12551
Diagonal (DIA)								
SP	2537.88	2745	208.11	11.97	569	0.64	17981	12.42
TCT	2537.88	2745	208.11	**1.88**	457	**0.68**	17981	**13.84**
BL	2537.89	2745	208.11	11.96	545	0.641	17981	12.41
HC	2537.89	2745	208.11	9.95	180	0.651	17981	12.7
LD	2537.89	2745	208.11	5.61	1091	0.681	17981	13.31
TrCT	2537.89	2745	208.11	2.34	2168	0.641	17981	13.71
SPTCT	2537.89	2745	208.11	13.81	1393	0.631	17981	12.15
BLTCT	2537.89	2745	208.11	2.29	2250	0.611	17981	13.78
HCTCT	2537.89	2745	208.11	9.08	1983	0.661	17981	12.81
Short Narrow (SN)								
SP	2591.88	2745	154.2	12.92	156	0.65	18260	12.36
TCT	2591.88	2745	154.2	**11.42**	161	**0.68**	18260	**12.57**
BL	2591.88	2745	154.2	14.50	56	0.64	18260	12.14
HC	2591.88	2745	154.2	13.73	100	0.64	18260	12.25
LD	2591.88	2745	154.2	14.43	81	0.63	18260	12.15
TrCT	2591.88	2745	154.2	15.20		0.65	18260	12.04
SPTCT	2591.88	2745	154.2	11.45	160	0.67	18260	12.57
BLTCT	2591.88	2745	154.2	11.45	160	0.67	18260	12.57
HCTCT	2591.88	2745	154.2	11.49	160	0.67	18260	12.56
Short Wide (SW)								
SP	2410	2745	336	25.68	106	0.51	17015	10.53
TCT	2410	2745	336	**24.15**	79	**0.54**	17015	**10.74**
BL	2410	2745	336	26.51	4	0.51	17015	10.41
HC	2410	2745	336	26.47	38	0.51	17015	10.41
LD	2410	2745	336	26.80	29	0.50	17015	10.37
TrCT	2410	2745	336	25.31	14	0.53	17015	10.58
SPTCT	2410	2745	336	24.19	160	0.53	17015	10.73
BLTCT	2410	2745	336	24.19	159	0.53	17015	10.73
HCTCT	2410	2745	336	24.19	160	0.53	17015	10.73
Long Narrow (LN)								
SP	2468	2745	278	15.24	42	0.60	17388	12.03
TCT	2468	2745	278	**9.89**	262	**0.65**	17388	**12.79**
BL	2468	2745	278	14.99	76	0.60	17388	12.07
HC	2468	2745	278	14.67	76	0.60	17388	12.11
LD	2468	2745	278	15.40	45	0.60	17388	12.01
TrCT	2468	2745	278	13.57	127	0.63	17388	12.27
SPTCT	2468	2745	278	13.70	109	0.62	17388	12.25
BLTCT	2468	2745	278	12.60	154	0.62	17388	12.41
HCTCT	2468	2745	278	13.70	109	0.62	17388	12.25
Long Wide (LW)								
SP	2190	2745	555	27.58	26	0.46	14580	10.88
TCT	2190	2745	555	**22.97**	162	**0.491**	14580	**11.57**
BL	2190	2745	555	26.62	51	0.46	14580	11.02
HC	2190	2745	555	26.39	69	0.46	14580	11.06
LD	2190	2745	555	24.84	142	0.47	14580	11.29

| Topology	Sum of Peak Powers under shading condition (W)	NO shading Array Maximum Power (W)	Shading Loss (W)	% Mismatch Loss (P_L)	Mis-leading Loss	Fill Factor (FF)	Input Insolation (P_{in}) = Insolation *area	Efficiency (η) =P_{mpp}/ P_{in}
TrCT	2190	2745	555	25.21	96	0.48	14580	11.23
SPTCT	2190	2745	555	25.84	79	0.47	14580	11.14
BLTCT	2190	2745	555	24.29	126	0.48	14580	11.37
HCTCT	2190	2745	555	25.84	79	0.47	14580	11.14
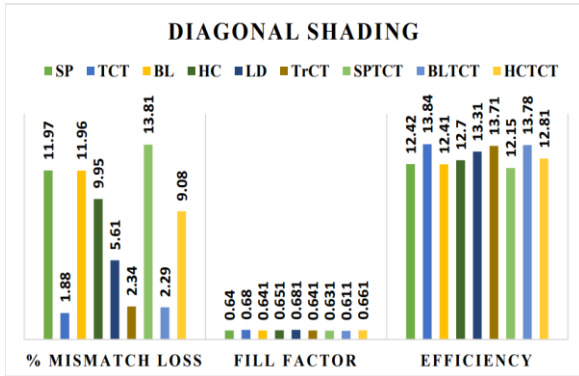
(a)
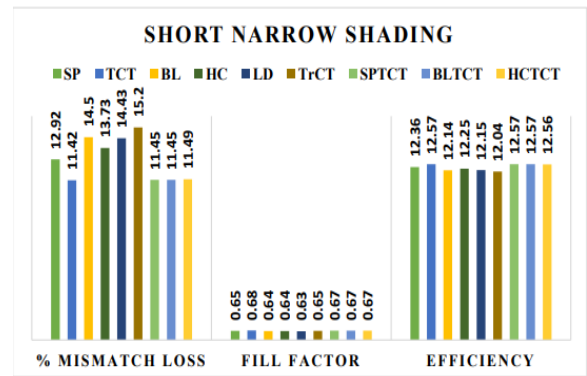
(b)
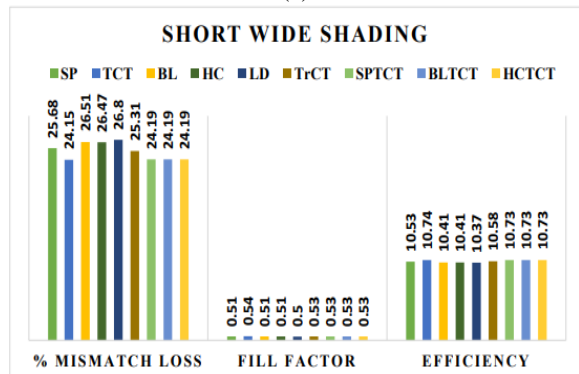
(c)
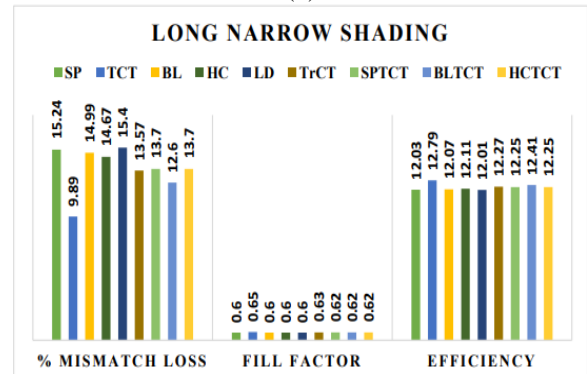
(d)
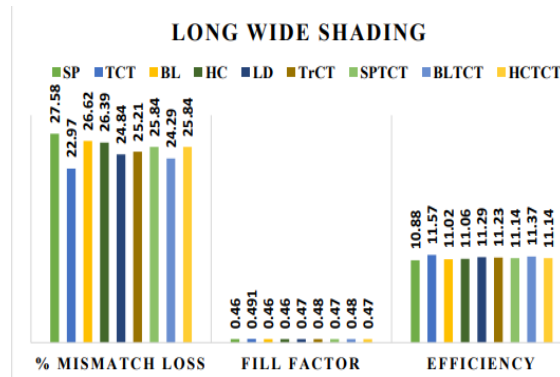
(e)

Figure 23. Comparative representation of conventional and hybrid configurations: (a) diagonal, (b) short narrow, (c) short wide, (d) long narrow, and (e) long wide

4.1 Payback time assessment of TCT configuration for Long Narrow (LN) Shading Condition:

The generated power in TCT = 2224 W
The generated power in SP = 2092 W
% Power gain = $\frac{((P_{max})_{TCT} - (P_{max})_{SP})}{(P_{max})_{SP}} \times 100$ = 6.3 %.

In a day, assuming a duration of partial shading = 4 hours, then Power saving per day = (2224 – 2092) * 4 = 0.528 kWh.

Then, the total units saved per annum ≈ 192.72 kWh = 193 units.

Compared to the SP topology, TCT requires 25 additional wires for a 6 x 6 array. Considering the length of one wire as 2 feet, the total required wire length is 50 feet, and the cost of one wire is taken as $1. Therefore, the total cost needed for the TCT configuration is $50.

Similarly, the cost per unit is considered as $0.107; then, the total units saved = $0.107 * 193 = $20.65.

Payback time in a year $= \frac{50}{21} = 2$ Years 5 months

A cost study shows that 25 additional TCT connections are needed to mitigate partial shading. These twenty-five extra connections cost $50 more than SP. Within 2 years and 5 months, a solar PV array with a 25-year lifespan returns more power than an SP array with long narrow shading, and Table 14 shows the payback times of conventional and hybrid configurations compared to TCT.

Table 14. Payback time of TCT Configuration compared to other topologies

Shading Pattern	Topology	% Power Enhancement	Payback Time
LN	SP	6.3	2 years 5 months
	BL	6	1 year 3 months
	HC	5.6	1 year 3 months
	LD	6.5	5 Months
	TrCT	4.3	4 Months
	SPTCT	4.4	1 year 4 months
	BLTCT	3.1	11 Months
	HCTCT	4.4	1 Year

5. CONCLUSIONS

This article delved into the assessment of passive techniques for mitigating the effects of partial shading in various shading scenarios. The subsequent analysis revealed the following observations:

In the DIA shading condition, the TCT configuration attains the highest power output of 2490 W. It also exhibits the lowest power loss due to mismatch at 1.88%, alongside optimal Fill-factor and efficiency values of 0.69 and 13.84, respectively. For SN, SW, and LW shading schemes, the differences in maximum power among all topologies are small, and TCT generates maximum power of 2296 W, 1828 W, and 1687 W, respectively.

In the LN shading condition, the TCT configuration achieves a peak power output of 2224 W, with a lowest mismatch power loss of 9.89%. Additionally, it attains an optimal Fill-factor of 0.64 and an efficiency of 12.8%. In conclusion, optimizing a photovoltaic (PV) array's maximum power potential can be achieved through reducing mismatch power loss or the number of series interconnections between individual modules. This study contributes to the design of PV module interconnections in densely populated areas by utilizing data related to peak power locations and shading factors. Additionally, optimal fill factor results from distributing shade uniformly across the entire string, as opposed to concentrating it in a singular spot. Ultimately, both the arrangement of the photovoltaic array and the manner in which shading is patterned and positioned significantly influence its overall effectiveness. When considering all the configurations, TCT exhibits the most favorable performance across a majority of shading conditions. Despite its higher initial expense due to increased interconnections among panels, this cost is recuperated in two years and five months.

6. ACKNOWLEDGEMENT

NOMENCLATURE

BL	Bridge Link
BLTCT	Bridge Link Total- cross – tied
HC	Honey Comb
HCTCT	Honey Comb Total- cross – tied
LD	Ladder
MPPT	Maximum Power Point Tracking
P	Parallel
PS	Partial Shading
PV	Photovoltaic
PVA	PV Array
S	Series
SP	Series Parallel
SPTCT	Series Parallel Total- cross – tied
TCT	Total- cross - tied
TrCT	Triple – cross - tied

REFERENCES

1. Belhachat, F. & Larbes, C. (2015). Modeling, analysis and comparison of solar photovoltaic array configurations under partial shading conditions. *Sol. Energy, 120, pp. 399–418.* https://doi.org/10.1016/j.solener.2015.07.039

2. Bhadoria, Singh, V., Pachauri, R. K., Tiwari, S., Jaiswal, S. P. & Alhelou, H. H. (2020). Investigation of different BPD placement topologies for shaded modules in a series-parallel configured PV array. *IEEE Access,8, 216911-216921.* https://doi.org/10.1109/ACCESS.2020.3041715

3. Bingol, O. & Ozkaya, B. (2018). Analysis and Comparison of different PV array configurations under partial shading conditions. *Solar Energy, 160, pp. 336-343.* https://doi.org/10.1016/j.solener.2017.12.004

4. Desai, A. A. & Mikkili, S. (2021). Comprehensive Analysis of Conventional and Hybrid PV Configurations Under Partial Shading Conditions to Mitigate Mismatching Loss and Optimize the Output Power. *Journal of Control, Automation and Electrical Systems, pp. 1-22,.* https://doi.org/10.1007/s40313-021-00800-2

5. Goud, J. S., Kalpana, R., Singh, B. & Kumar, S. (2018). A global maximum power point tracking technique of partially shaded photovoltaic systems for constant voltage applications. *IEEE Transactions on Sustainable Energy, 10(4), 1950-1959.* https://doi.org/10.1109/TSTE.2018.2876756

6. Husain, A. A .F., Hasan,W. Z. W., Shafie, S, Hamidon, M. N. & Sudhir Pandey, Sh. (2018). A review of transparent solar photovoltaic technologies. *Renewable and sustainable energy reviews, 94: 779-791.* https://doi.org/10.1016/j.rser.2018.06.031

7. Kumar Varma, H., Reddy Barry, G. V. & Kumar Jain, R. (2021). A Novel Magic Square Based Physical Reconfiguration for Power Enhancement in Larger Size Photovoltaic Array. *IETE Journal of Research, 69(7), 1-14.* https://doi.org/10.1080/03772063.2021.1944333

8. Kang Kho, C. T., Ahmed, J., Then, Y. L. & Kermadi, M. (2018). Mitigating the effect of partial shading by triple-tied configuration of PV modules. *In 2018 IEEE PES Asia-Pacific Power and Energy Engineering Conference (APPEEC), pp. 532-537. IEEE,* https://doi.org/10.1109/APPEEC.2018.8566375

9. Krishna, S. G., & Moger, T. (2019). Optimal SuDoKu reconfiguration technique for total-cross-tied PV array to increase power output under non-uniform irradiance. *IEEE Transactions on Energy Conversion, 34(4), 1973-1984.* https://doi.org/10.1109/TEC.2019.2921625

10. Premkumar, M., Subramaniam, U., Babu, T.S., Elavarasan, R.M. & Mihet-Popa, L. (2020) Evaluation of mathematical model to characterize the performance of conventional and hybrid PV array topologies under static and dynamic shading patterns. *Energies, 13(12), p.3216.* https://doi.org/10.3390/en13123216

11. Pendem, S. R. & Mikkili, S. (2018). Modelling and performance assessment of PV array topologies under partial shading conditions to mitigate the mismatching power losses. *Solar Energy, 160, pp. 303-321,* https://doi.org/10.1016/j.solener.2017.12.010

12. Suresh, H.N., Rajanna, S., Thanikanti, S.B. & Alhelou, H.H. (2022). Hybrid interconnection schemes for output power enhancement of solar photovoltaic array under partial shading conditions. *IET Renewable Power Generation.* *https://ietresearch.onlinelibrary.wiley.com/doi/full/10.1049/rpg2.12543*

13. Tatabhatla, V. M. R., Agarwal, A. & Kanumuri, T. (2019). Improved power generation by dispersing the uniform and non-uniform partial shades in solar photovoltaic array. *Energy Conversion and Management, 197 (2): 111825.* https://doi.org/10.1016/j.enconman.2019.111825

14. Zhou, G., Tian, Q., Leng, M., Fan, X. & Bi, Q. (2020). Energy management and control strategy for DC microgrid based on DMPPT technique. *IET Power Electronics, 13(4): 658-668.* https://doi.org/10.1049/iet-pel.2019.0383